



TRC9901

Permeability of Superpave

Kevin D. Hall, Josue Cruz, Hooi Gin

Final Report

2004

FINAL REPORT

TRC-9901
Permeability of Superpave

by

Kevin D. Hall, Josue Cruz, and Hooi Gin

conducted by

Department of Civil Engineering
University of Arkansas

in cooperation with

Arkansas State Highway and Transportation Department

U.S. Department of Transportation
Federal Highway Administration

University of Arkansas
Fayetteville, Arkansas 72701

March 2004

ACKNOWLEDGMENTS / DISCLAIMER

This report is based on the findings of Project TRC-901, Permeability of Superpave.

TRC-9901 is sponsored by, and this report is prepared in cooperation with, the Arkansas State Highway and Transportation Department and the U.S. Department of Transportation, Federal Highway Administration.

The contents of this report reflect the views of the authors who are responsible for the facts and the accuracy of the data presented herein. The contents do not necessarily reflect the official views or policies of the Arkansas State Highway and Transportation Department or the Federal Highway Administration. This report does not constitute a standard, specification, or regulation.

SI CONVERSION FACTORS

$$1 \text{ inch} = 25.4 \text{ mm}$$

$$1 \text{ foot} = 0.305 \text{ m}$$

$$1 \text{ lb/ft}^3 = 16 \text{ kg/m}^2$$

$$1 \text{ psi} = 6.9 \text{ kN/m}^2$$

$$1 \text{ lb} = 4.45 \text{ N}$$

TABLE OF CONTENTS

Chapter 1 - Introduction	1
Chapter 2 – Background and Literature Review	4
Chapter 3 – Research Approach	30
Chapter 4 – Test Results and Discussion	40
Chapter 5 – Conclusions and Recommendations	59
References	62
Appendix A: Mix Properties	65
Appendix B: Specimen Preparation and Permeability Test Instructions	69
Appendix C: Laboratory Performance Testing Using ERSA	77

LIST OF TABLES

Table 1. Variation of $\eta_c / \eta_{20^\circ\text{C}}$ for Permeability Calculations	9
Table 2. Location and number of SGC samples used for testing	39
Table 3. Location and number of Field Cores used for testing	39
Table 4. Summary of Permeability versus Air Voids Models	41
Table 5. ANOVA Results for Confining Pressure Evaluation	48
Table 6. ANOVA Results for Testing Time Evaluation	50
Table 7. Water Collected for Phase I Falling Head Tests	52
Table 8. ANOVA Results for Initial Hydraulic Gradient Evaluation	53
Table 9. Effect of Initial Hydraulic Gradient on Permeability	54

LIST OF FIGURES

Figure 1. Pavement Structure “Weeping” Moisture	2
Figure 2. Darcy’s Experiment Setup	5
Figure 3. Flow Zones	5
Figure 4. Constant Head Permeability Test	10
Figure 5. Falling Head Permeability Test	11
Figure 6. Falling Head/ Rising Tail Test Assembly	13
Figure 7– Water Permeability Laboratory Testing Apparatus	15
Figure 8– Water Permeability Laboratory Testing schematic (ASTM PS 129-01)	16
Figure 9. Severely Stripped ACHM Specimen	18
Figure 10. ACHM Pavement Showing Severe Ravelling	18
Figure 11. Effects of Oxidation on ACHM	19
Figure 12. Plot of % Air Voids vs. Log Permeability. (8)	21
Figure 13. Pavement Air Flow Rates Used to predict Relative Density of Cores. (9)	22
Figure 14. Air Flow Rate / Mix Temperature Relationship. (9)	22
Figure 15. Darcy’s Law Validation: Hydraulic Gradient / Rate of Flow Relationship (10)	23
Figure 16. Florida DOT Permeability Test results. (15)	27
Figure 17. Comparison of the Karol-Warner and FDOT Permeameters. (15)	27
Figure 18. Falling head/ Rising Tail Test Permeameter Assembly	34
Figure 19. Schematic of the Falling Head/Rising Tail Test	35
Figure 20. Relationship Between Air Voids and Permeability – All Samples	40
Figure 21. Typical ERSA Output	42
Figure 22. ERSA Results: 12.5 mm Laboratory Samples	43

LIST OF FIGURES (Continued)

Figure 23. ERSA Results: 12.5mm Field Cores	44
Figure 24. ERSA Results: 25 mm Field Cores	45
Figure 25. Relationship Between ERSA Rut Depth and Permeability, 12.5 mm Laboratory Samples	46
Figure 26. Relationship Between ERSA Rut Depth and Permeability, 12.5 mm Field Cores (Hartford AR 45)	46
Figure 27. Relationship Between ERSA Rut Depth and Permeability, 12.5 mm Field Cores (Mt. Home By-Pass)	47
Figure 28. Relationship of Permeability to Testing Time (typical)	52
Figure 29. Effect of Soaking Period on Degree of Saturation	56
Figure 30. Effect of Saturation on Hydraulic Conductivity – Low Voids	57
Figure 31. Effect of Saturation on Hydraulic Conductivity – Medium Voids	58
Figure 32. Effect of Saturation on Hydraulic Conductivity – High Voids	58

CHAPTER 1

INTRODUCTION

Historically most states in the country (including Arkansas) used the Marshall method of mix design for the construction of their asphalt concrete hot mix (ACHM) pavements. Mixes designed using the Marshall procedure tended to be relatively dense graded; surface mixes in particular tended to compact tightly and exhibit low in-place permeability. A new method of mix design was developed in the early 1990's as a result of research initiated by the Strategic Highway Research Program (SHRP). This new method, termed "Superpave" (Superior Performing Asphalt Pavements), consisted of three primary products: (1) a performance-related binder specification; (2) procedures that seek both the "best" aggregate structure using available aggregates and the optimum binder content for that design aggregate structure; and (3) a set of performance-related mixture tests. The Arkansas State Highway and Transportation Department (AHTD) placed its first Superpave ACHM in a test section in 1995; by 1998 all ACHM used on pavements included in the interstate, national highway system, and state highway system in Arkansas was designed using Superpave specifications.

Superpave gradation criteria tend to produce relatively coarse and slightly open-graded ACHM compared to traditional AHTD mixes designed using the Marshall method. The relative open nature of ACHM mixes designed using Superpave, and observations by the AHTD and contractor personnel of moisture in Superpave binder and surface mixes, gave rise to concerns regarding the permeability of Superpave mixes. Figure 1 shows moisture "weeping" from a pavement structure consisting of a Superpave overlay of an existing flexible pavement designed using the Marshall system.



Figure 1. Pavement Structure “Weeping” Moisture

High ACHM permeability allows moisture to percolate into the pavement structure. The presence of this moisture may, in turn, lead to serious problems in pavement performance, including saturation of base and subgrade layers, increased oxidation of the asphalt binder, and entrapment of water within the ACHM. (1) Premature pavement failures on Superpave pavements could seriously undermine the traveling public’s confidence in Superpave.

To ensure successful implementation of Superpave in Arkansas, AHTD addressed the concern over ACHM permeability by sponsoring research project TRC-9901, “Permeability of Superpave”. The primary objective of the research was to develop strategies for considering ACHM permeability during design and/or construction. Implementation of such strategies could include test specifications for determining the permeability of ACHM; design policies for increasing the drainage ability of the pavement structure; revised ACHM material specifications regarding gradation or other properties; and/or construction guidelines/specifications regarding

field density requirements. A number of specific objectives to be met in the study were identified, as summarized below:

- Fully document potential pavement problems caused by excess moisture.
- Develop routine testing protocols for determining the permeability of ACHM.
- Establish relationship between ACHM permeability and mixture performance.
- Develop specific methodologies for considering permeability in design and construction.

This report contains the results obtained on project TRC-9901. The literature review provides complete documentation of the distress mechanisms related to moisture and air infiltration that affect constructed pavements. The research and experimental phases include testing protocols recommended for determining the hydraulic conductivity (permeability) of ACHM, as well as attempts to correlate permeability to pavement performance and ACHM volumetric properties. They also provide guidance for considering the apparent increase in permeability of ACHM associated with Superpave mixes. All research was performed at the Department of Civil Engineering at the University of Arkansas, Fayetteville.

CHAPTER 2

BACKGROUND AND LITERATURE REVIEW

Permeability can be defined as the ability of a porous medium to allow the flow of a fluid through it, typically expressed as the coefficient of hydraulic conductivity, (k). A porous medium is a material, granular or fibrous, containing void spaces. (2) The fluid may be either a liquid or a gas. In this particular project, the medium studied was Superpave designed asphalt mixtures and the fluid used was distilled water at room temperature. It is useful to thoroughly review the theory behind the calculation of permeability, and previous work regarding the measurement of permeability for asphalt mixes in order to assess the validity of the experiments executed during the completion of the project.

Permeability Theory - Darcy's Experiment

The theory of laminar flow through porous media is based on a classical experiment originally performed by Darcy in Dijon, France. He applied Bernoulli's fluid mechanics equation to the flow of water through a porous soil medium. According to Bernoulli's equation, the total head at a point in water under motion can be given by the sum of the pressure head (u/γ_w), velocity head ($v^2/2g$), and elevation head (Z). However seepage velocity is negligible. (3)

Figure 2 shows the relationship among pressure, elevation, and total heads for the flow of water through soil. Open standpipes called piezometers are installed at points A and B. The levels to which water rises in the piezometer tubes situated at points A and B are known as the piezometric levels of points A and B, respectively. The pressure head at a point is the height of the vertical column of water in the piezometer installed at that point.

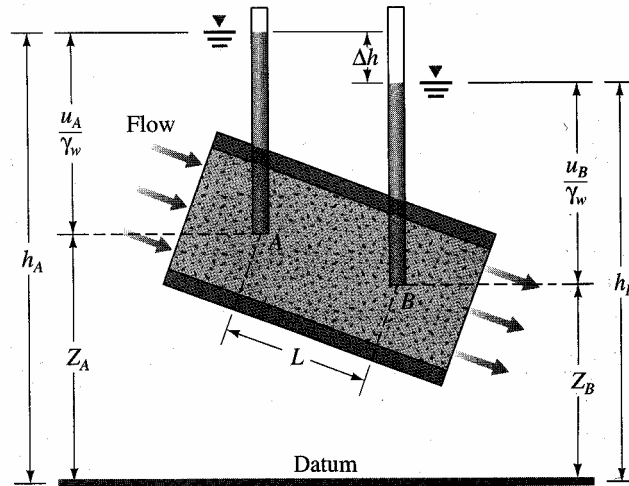


Figure 2. Darcy's Experiment Setup

In general, the variation of the velocity, v , with the hydraulic gradient, I , is as shown in Figure 3. This relationship is divided into three zones:

- 1) Laminar flow zone (I)
- 2) Transition zone (II)
- 3) Turbulent flow zone (III)

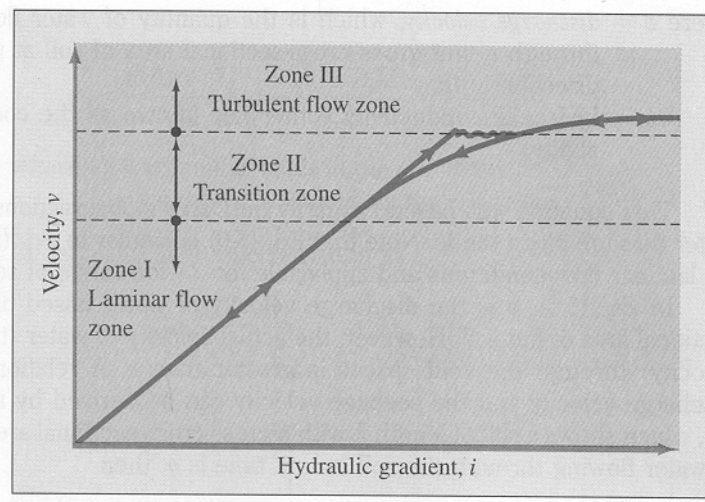


Figure 3. Flow Zones

When the hydraulic gradient is gradually increased, the flow remains laminar in zones I and II, and the velocity, v , bears a linear relationship to the hydraulic gradient. At a higher hydraulic gradient, the flow becomes turbulent (Zone III). When the hydraulic gradient is decreased, laminar flow conditions exist in zone I only. In fractured rock, stones, gravels, very coarse sands, and other granular materials, turbulent flow conditions may exist and a linear relationship between the velocity and hydraulic gradient cannot be established.

Darcy showed that under steady conditions of flow through beds of sand of various thicknesses and under various pressures, the rate of flow was always proportional to the hydraulic gradient (i), i.e. to the fall in hydraulic head per unit thickness of sand. In 1856, he published a simple equation for the discharge velocity of water through saturated soils, which may be expressed as

$$v = ki = \frac{\Delta h}{l} k \quad \text{Equation 1}$$

where:

v = discharge velocity (quantity of water flowing in unit time through a unit gross cross-sectional area of a porous material at right angles to the direction of flow)

Δh = head loss

l = length of the specimen

k = hydraulic conductivity (otherwise known as the coefficient of permeability)

and

$$i = \frac{\Delta h}{l} \quad \text{Equation 2}$$

which is the hydraulic gradient (ratio between the head loss and length of specimen across which the head loss occurred).

This principle, known as Darcy's Law, has been found to be generally valid for the flow of water through all soils. Although Equations 1 and 2 were based primarily on Darcy's observations about the flow of water through clean sands, it is valid only for laminar flow

conditions but applicable for a wide range of granular materials. However, it does have limitations. According to Leonards, the following assumptions must be met for Darcy's Law to apply (4):

- 1) The material in question must be homogeneous and porous.
- 2) Continuous, saturated, two-dimensional flow must be present.
- 3) The flow fluid must be homogeneous.
- 4) Steady state flow conditions.
- 5) The fluid must be incompressible.

Hydraulic conductivity is generally expressed in SI units and, for scale convenience, multiplied by 10^5 . In this way, the value is given as $Y \times 10^{-5}$ cm/sec. The hydraulic conductivity of asphalt mixtures and other mediums depends on several factors: fluid viscosity, air voids, pore-size distribution (void connectivity), grain-size distribution, roughness of particles, and degree of saturation. Generally, permeability increases with an increase in air voids, void connectivity, and degree of saturation. Permeability decreases with an increase in fluid viscosity and particle roughness. (3) The hydraulic conductivity of a soil is also related to the properties of the fluid flowing through it by the following equation:

$$k = \frac{\gamma_w}{\eta} \bar{K}$$

Equation 3

where:

γ_w = the unit weight of water

η = the viscosity of water

\bar{K} = is the absolute permeability (expressed in units of L^2 , such as cm^2 , ft^2 , etc.)

From Equation 3, it is readily noticeable that hydraulic conductivity is a function of the unit weight and viscosity of water. For this reason careful monitoring of water temperature is needed when testing for permeability of materials. However, water being used for permeability testing may be at any temperature, but proper correction factors must be included to account for changes in water properties. The following equation should be used for this purpose.

$$\frac{k_{T_1}}{k_{T_2}} = \left(\frac{\eta_{T_2}}{\eta_{T_1}} \right) \left(\frac{\gamma_{w(T_1)}}{\gamma_{w(T_2)}} \right) \quad \text{Equation 4}$$

where:

k_{T_n} = hydraulic conductivity at temperature T_n .

η_{T_n} = viscosity of water at temperature T_n .

$\gamma_{w(T_n)}$ = unit weight of water at temperature T_n .

It is conventional to express the value of k at a temperature of 20° C. Within the range of test temperatures it can be assumed that the unit weight of water is constant. However, this is not the case for values of water viscosity. Table 1 shows the variation of water viscosity with respect to temperature.

All the principles that have been presented form part of the most fundamental principles of soil mechanics. Application of these principles has been extended to encompass asphalt pavement mixture permeability. In the next section, a review of permeability test methods and their application to ACHM is presented.

Temperature, T (°C)	$\eta_{°C} / \eta_{20°C}$
15	1.135
16	1.106
17	1.077
18	1.051
19	1.025
20	1.000
21	0.976
22	0.953
23	0.931
24	0.910
25	0.889
26	0.869
27	0.850
28	0.832
29	0.814
30	0.797

Table 1. Variation of $\eta_{°C} / \eta_{20°C}$ for Permeability Calculations.

Laboratory Permeability Tests

Two standard laboratory tests are used to determine the hydraulic conductivity of soil: the constant head test and the falling head test. A brief description of each test type follows.

Constant Head Test

A typical arrangement of the constant head permeability test is shown in Figure 4. In this type of laboratory setup, the water supply at the inlet is adjusted in such a way that the difference of head between the inlet and the outlet remains constant during the test period. After a constant flow rate is established, water is collected in a graduated flask for known time duration.

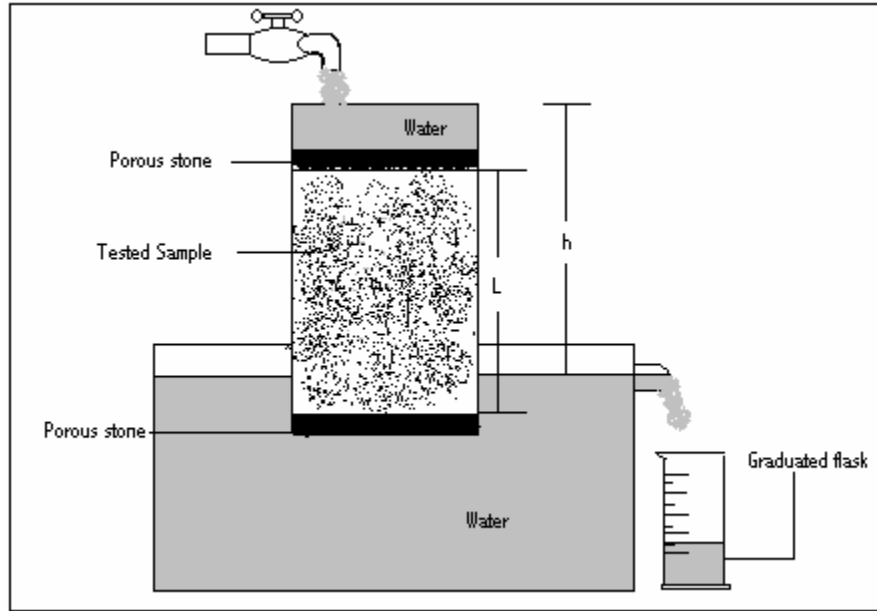


Figure 4. Constant Head Permeability Test

For the constant head test, the total volume of water collected may be expressed as shown in Equation 6.

$$Q = Avt = A(ki)t \quad \text{Equation 6}$$

and since (from Equation 2),

$$i = \frac{\Delta h}{l}$$

a substitution of Equations 2 and 6 yields

$$Q = At \left(k \frac{h}{l} \right) \quad \text{Equation 7}$$

or

$$k = \frac{Ql}{Aht} \quad \text{Equation 8}$$

where:

Q = volume of collected water

A = cross sectional area of the specimen

t = duration of water collection

l = length of the specimen

No constant head tests were performed during this research project. Previous work regarding permeability testing of asphalt mixtures concluded that there is no statistical difference between a constant head and falling head test. (5) One particular study concluded that a constant head permeability test is the equivalent of running an infinite number of falling head tests with an infinitely small head loss. (6)

Falling Head Test

A typical arrangement of the falling head permeability test is shown in Figure 5. Water from a standpipe flows through the sample. The initial head difference, h_1 , at time $t=0$ is recorded, and water is allowed to flow through the soil specimen such that the final head difference at time $t = t_2$ is h_2 .

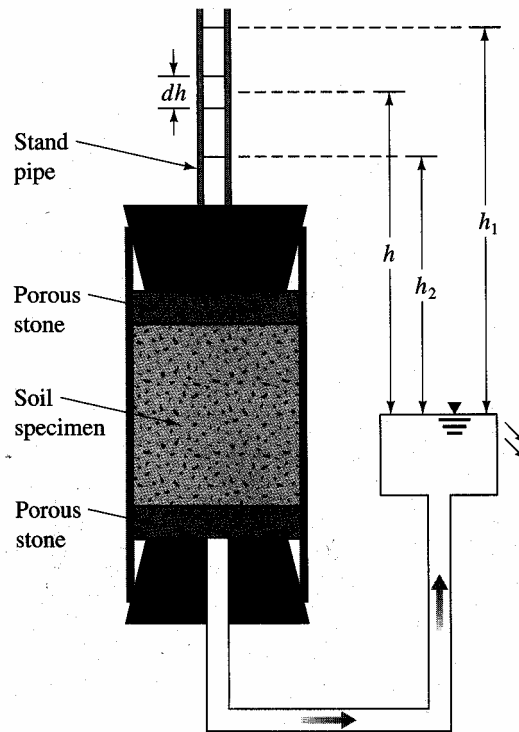


Figure 5. Falling Head Permeability Test

The rate of flow of the water through the specimen at any time “t” is given by Equation 9:

$$q = kA \frac{h}{l} = -a \frac{\Delta h}{\Delta t} \quad \text{Equation 9}$$

Rearrangement of Equation 9 yields

$$dt = \frac{al}{Ak} \left(\frac{-dh}{h} \right) \quad \text{Equation 10}$$

Integration of the left side of Equation 10 with limits of time from 0 to t and the right side with limits of head difference from h_1 to h_2 gives

$$t = \frac{al}{Ak} \ln \left(\frac{h_1}{h_2} \right) \quad \text{Equation 11}$$

Solving Equation 11 and changing the logarithmic base produces Equation 12:

$$k = 2.303 \frac{al}{At} \log_{10} \left(\frac{h_1}{h_2} \right) \quad \text{Equation 12}$$

where:

q = flow rate

A = cross-sectional area of the sample

a = cross-sectional area of the standpipe

Equation 12 was used in all permeability calculations related to falling-head tests conducted during this research project.

Falling Head, Rising Tail Test

This test was initially investigated for two primary reasons. First, the calculated permeability values for samples tested using this setup, as well as the permeameter assembly and process itself is easily checked for consistency. Secondly, the validity of Darcy’s Law for the test executed in the laboratory can be evaluated. It was initially assumed for the tests that Darcy’s law is valid and that the hydraulic conductivity is essentially unaffected by hydraulic gradient. The falling head, rising tail test allows the hydraulic conductivity of specimens to be measured at

three hydraulic gradients. If all measured values are similar (within about 25%) then Darcy's law may be taken as valid. (7) A typical permeameter assembly used for this setup is shown in Figure 6.

The following equation was used in all calculations of permeability values for samples tested with the falling-head/rising-tail setup:

$$k = \frac{a_{in} a_{out} L}{At(a_{in} + a_{out})} \ln\left(\frac{h_1}{h_2}\right) \quad \text{Equation 13}$$

where:

a_{in} = cross-sectional are of the reservoir containing the influent water

a_{out} = cross-sectional area of the reservoir containing the effluent water

L = length of the specimen

A = cross-sectional area of the specimen

t = elapsed time between determination of h_1 and h_2

h_1 = head loss across the specimen at time t_1

h_2 = head loss across the specimen at time t_2 .

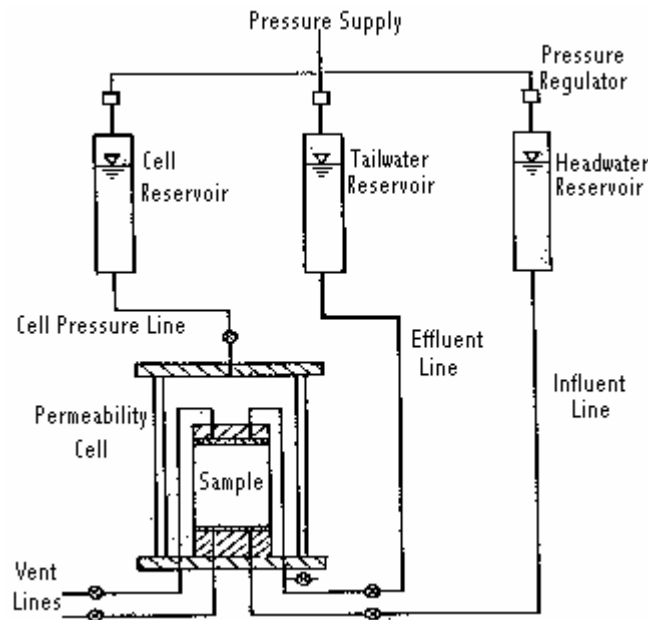


Figure 6. Falling Head/ Rising Tail Test Assembly

Falling Head, Constant Tail Test

Figure 7 shows a water permeability laboratory testing apparatus based on the principle of a falling-head constant-tail permeability test. Figure 8 is a schematic of the testing setup. The basic principle of the falling-head constant-tail test is similar to other falling-head tests. The apparatus and testing procedure are detailed in ASTM PS 129-01. In this test, the coefficient of water permeability through the specimen is calculated according to Equation 14.

$$k = \frac{a * l}{A * t} \ln \left(\frac{h_1}{h_2} \right) \quad \text{Equation 14}$$

Where :

k = coefficient of water permeability, cm/s,

a = inside cross-sectional area of inlet standpipe, cm²,

l = thickness of test specimen, cm,

A = cross-sectional area of test specimen, cm²,

t = average elapsed time of water flow between timing marks, s,

h₁= hydraulic head on specimen at time t₁, cm, and

h₂= hydraulic head on specimen at time t₂, cm.

Some key assumptions regarding this calculation of permeability include:

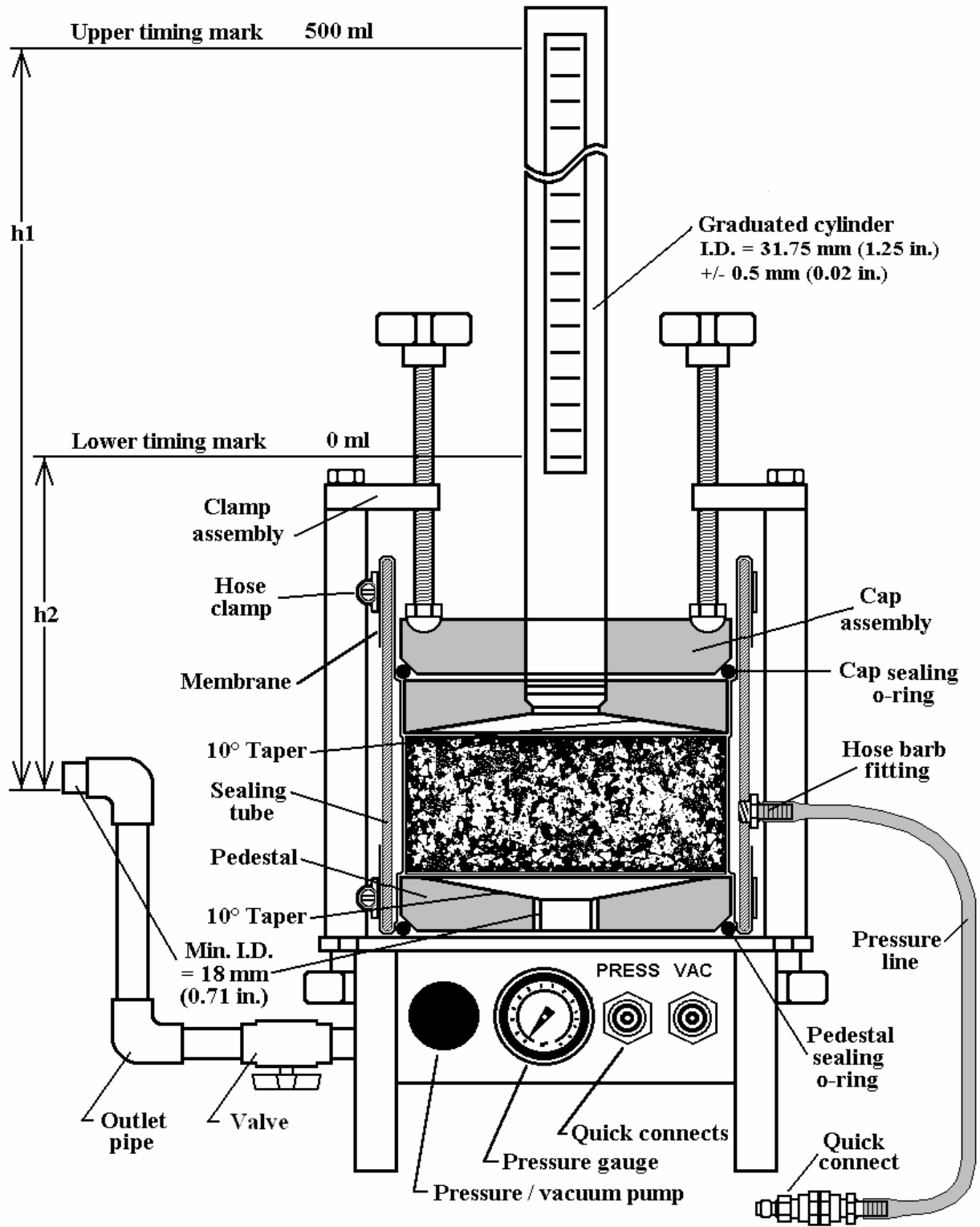
1. Flow of water is laminar,
2. Permeability is unaffected by hydraulic gradient
3. Darcy's law is valid.

As with other falling-head type tests, questions concerning the validity of the key assumptions have been raised; however, test results reported in the literature give credence to the effectiveness of this testing approach.



Figure 7– Water Permeability Laboratory Testing Apparatus

Figure 8– Water Permeability Laboratory Testing schematic (ASTM PS 129-01).



Test Selection

ASTM Committee D-04 (specifically subcommittee 4-23) sponsored a task group whose mission was to investigate the development of a relatively simple, inexpensive, yet accurate method for consistently measuring ACHM permeability in the laboratory. The task group included personnel from the Virginia Transportation Research Council, the Florida Department of Transportation, the National Center for Asphalt Technology, APAC Materials Services, and the University of Arkansas (the TRC-9901 team). The task group initially suggested a “standard” falling-head test, considering that test to be the most easily adaptable to a variety of laboratory conditions.

Potential Effects of Increased Permeability on Pavement Performance

Comprehension of the significance of pavement permeability justifies the extensive testing performed in this research project. Essentially all ACHM pavements are permeable to a certain extent. However, it is important that permeability be within certain limits to ensure the durability of the compacted mix. Water, and to a lesser extent, air intrusion into an asphalt pavement can lead to serious performance problems. Such problems can include:

Stripping: This refers to a phenomenon which takes place in an asphalt bound layer whereby the presence of a prolonged high-moisture condition (together with an aggregate with a high-stripping potential) leads to the debonding of the asphalt binder from the aggregate particles. This loss of bond reduces the ability of the asphalt bound layer to carry tensile strains and generally reduces the overall load-carrying capacity of the pavement. Figure 9 shows an ACHM specimen that has experienced severe stripping.

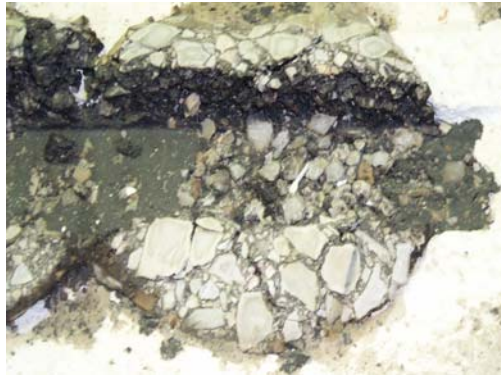


Figure 9. Severely Stripped ACHM Specimen.

In severe cases of stripping the ACHM or asphalt bound layer stops behaving like a bound layer and actually behaves more like an unbound layer. (*I*) Stripping can lead to drastic pavement failures in terms of rutting, cracking, and raveling (Figure 10).



Figure 10. ACHM Pavement Showing Severe Ravelling.

Freeze-thaw damage: saturated pavements, if frozen, could develop significant cracking and raveling as a result of water freezing and swelling in the pore spaces of the surface and binder mix.

Base saturation: intrusion of water into the pavement may seriously weaken layers underlying the ACHM surface (e.g. unbound granular base, subgrade), leading to serious and premature structural (load-associated) failures such as rutting and fatigue cracking.

Oxidation: asphalt cement reacts with oxygen in the air (oxidation) and hardens over time. Pavements with oxidized asphalt cement binder are susceptible to cracking and deterioration resulting from loads and/or environment as the binder becomes increasingly brittle. This process is accelerated when a larger percentage of the coated aggregates in a bituminous mix is exposed to air, such as in the case of a pavement exhibiting relatively high permeability. Figure 11 illustrates a heavily oxidized HMA surface layer.



Figure 11. Effects of Oxidation on ACHM

Past Investigations of ACHM Permeability

McLaughlin and Goetz (1955)

In 1955 McLaughlin and Goetz presented a report to the Highway Research Board. (8) Within this report they attempted to correlate permeability and void content of asphalt pavement mixtures to durability by designing, constructing, and operating testing equipment for measuring

permeability. They hypothesized that permeability is a better measure of durability than is void content. Permeability, they contended, measures the capacity of the porous material to transmit fluid, which relates directly to the forces that produce disintegration.

The scope of their research may be summarized in the following statements. However, it is important to note that they did not intend to give the status of final conclusions to these enumerated statements, since they were well aware of the limited amount of data they analyzed.

(8)

- 1) The results of tests performed using a designed permeameter (one that employs compressed air for measuring the permeability of bituminous-aggregate mixtures) were found to be in agreement with tests made with conventional falling-head water permeameters.
- 2) A relationship between voids and permeability was found which agrees with previous work on soils and other materials. A plot of voids versus log permeability is essentially linear (refer to Figure 12). For bituminous mixtures this relationship is influenced by such factors as gradation of the aggregate, compaction, and the amount of asphalt in the mixture.
- 3) The relationship between voids and permeability for bituminous concrete of the range investigated is influenced to a large degree by asphalt content. At higher asphalt contents permeability is much more sensitive to changes in void content than it is at lower asphalt contents.
- 4) There is no relationship between permeability and durability as measure by percent loss in sonic modulus caused by laboratory freezing and thawing.

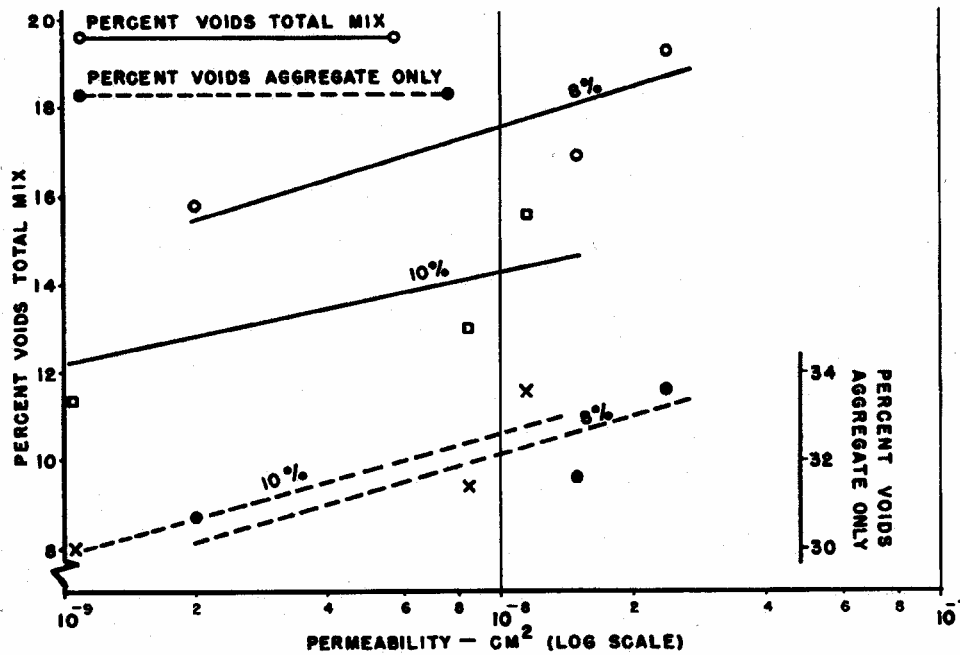


Figure 12. Plot of % Air Voids vs. Log Permeability. (8)

Hein and Schmidt (1961)

After conducting a study on air permeability of asphalt concrete, Hein and Schmidt suggested that permeability measurements are essential to routine mix design studies. (9) Their results indicated that the void content of mixtures is not necessarily proportional to permeability when the variation is caused by gradation. Two very important conclusions they reached are that pavement air flow rates measured in the field may be used to predict relative density of cores (Figure 13) and that the air flow rate through a pavement depends on the mix temperature (Figure 14). Hein and Schmidt also concentrated on effects of construction techniques on permeability measured on in-place pavements. Their work essentially confirmed in the field what McLaughlin and Goetz (8) had shown in the laboratory.

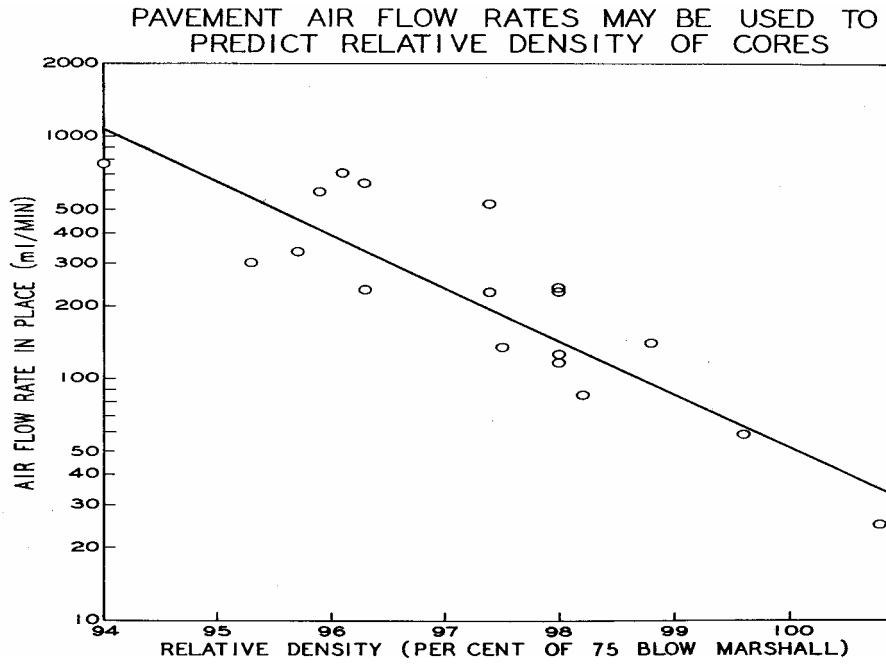


Figure 13. Pavement Air Flow Rates Used to predict Relative Density of Cores. (9)

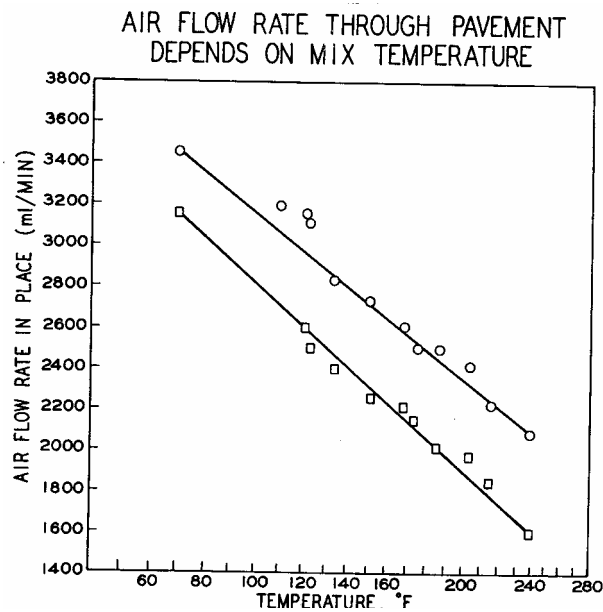


Figure 14. Air Flow Rate / Mix Temperature Relationship. (9)

Shklarsky and Kimchi (1962)

Shklarsky and Kimchi studied permeability of sand asphalt mixtures using waters as the flow medium in an attempt to prove the validity of Darcy's law applied to bituminous mixtures. From the limited results of their study they drew the following conclusions (10):

- 1) Permeability shows a linear relationship between the hydraulic gradient and rate of water flow, thus proving Darcy's law is valid (please refer to Figure 15).

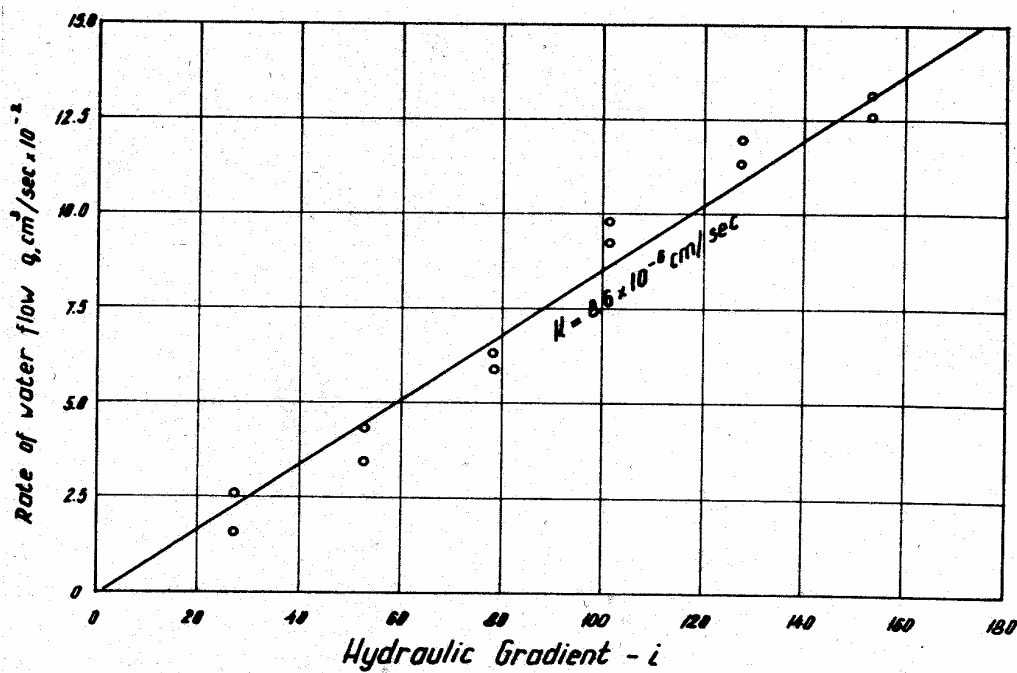


Figure 15. Darcy's Law Validation: Hydraulic Gradient / Rate of Flow Relationship (10)

- 2) At the beginning of their tests, the rate of flow of water was high; on repeating the test, a gradual decrease was observed tending to a constant limit.
- 3) The bitumen and filler contents of the asphalt mixtures tested affect the coefficient of permeability indirectly.

Kumar and Goetz (1977)

Kumar and Goetz developed an “improved” method for measuring permeability on compacted bituminous mixtures that greatly increased accuracy and reduced variability. Their equipment was the forerunner of the device required in a “standardized” test for measuring permeability of asphalt concrete, detailed in ASTM D3637-84. However, most materials engineers and researchers found the requirements and device described in the ASTM standard unnecessarily complicated. Subsequently the ASTM standard was discontinued. Many agencies continued to experiment with, and fabricate their own, devices for measuring permeability. In fact, one 1986 study found nine different types of permeameters used in the laboratory. At the time of this research, no single standard test existed to consistently measure the permeability of compacted asphalt concrete specimens.

McWilliams (1986)

The AHTD sponsored research aimed at relating measured permeability to bituminous mixture properties. For the study, a permeameter was constructed that could be used to measure the permeability of a compacted specimen using both air and water as the flow medium. Some conclusions from the study follow. *(II)*

- 1) Air and water permeability, although related, are not quantifiably identical. Data suggests that a given asphalt mixture is up to 150 times less permeable to water than air.
- 2) Aggregate gradation dictates the size and shape of the void structure in a given asphalt mixture; therefore, individual gradations have unique permeability characteristics.
- 3) Increased compactive effort typically achieves a more uniform and well-defined aggregate structure, which leads to less variability in permeability from sample to sample.
- 4) The amount of mineral filler and relatively fine sand drastically reduces both air and water permeability.

Relationship(s) Between Permeability and ACHM Properties

Little was done in the Arkansas study to relate specific levels of permeability to field performance. In fact, very little data is available that relates field performance to measured mix permeability. Historically, relationships between field performance and permeability have used an “intermediary” such as air voids- relating performance to constructed in-place voids, and relating measured permeability to compacted voids. These inferred relationships between permeability and void content are neither well documented nor validated. Nevertheless, permeability is thought to be related to the amount and structure of the air voids present in a compacted mixture. (12)

In the early 1960’s, Zube showed that for dense-graded ACHM mixes, pavements become excessively permeable to water at approximately 8 percent air voids. (13) This observation was confirmed in 1989 by Brown, Collins, and Brownfield. They reported that Georgia ACHM mixtures remained relatively impermeable to water when void contents remained below 8 percent. (14) Recent studies conducted using stone-matrix asphalt (SMA) mixes suggest the “critical” air void level with respect to permeability to be approximately 6 to 7 percent. Some studies in Florida using relatively open-graded Superpave ACHM also suggest 6 to 7 percent voids as a maximum to limit permeability potential. (15)

Florida Investigations of Water Permeability of Coarse Graded Superpave Pavements

One of the earliest attempts to respond to detrimental levels of permeability in Superpave mixes occurred in Florida. Field personnel in Florida reported instances of moisture “weeping” from completed Superpave pavements, giving rise to concern over moisture-related problems with pavement performance. (16) Subsequent investigation revealed that many “bathtub” sections were being constructed, in which a highly-permeable Superpave mix was being placed

on an asphalt-rubber (relatively impermeable) interlayer base and surrounded by relatively dense-graded (Marshall designed) asphalt concrete shoulders. Moisture infiltrating the Superpave mix was literally trapped.

The Florida Department of Transportation (FDOT) responded by introducing a number of specifications aimed at reducing the potential for moisture-related damage to new asphalt mixes with relatively high permeability. These specifications took the following forms (15):

- 1) *Permeability test*: Florida developed a modified falling head permeability test for asphalt concrete. The initial version of the test used an epoxy coating to seal the edges of a field specimen (6 inches in diameter and 2 inches thick) against a rigid-wall permeameter. However, subsequent studies have been performed using a Karol-Warner flexible-wall permeameter (identical to the device currently being investigated by the ASTM D4-23 task group) for simplicity.
- 2) *Permeability requirements*: Florida specifications target 100×10^{-5} cm/sec as the maximum permeability for bituminous mixtures. Some limited studies done in Florida suggest that this level of permeability corresponds to approximately 6 percent air voids in a compacted mixture. Figure 16 shows the Florida test results that form the basis for the permeability specification. The 100×10^{-5} cm/sec specification was developed from tests using the initial “rigid wall” permeameter. Subsequent studies using the Karol-Warner flexible wall device (Figure 17) suggest that the specification should be changed to 125×10^{-5} cm/sec for compatibility with the 6 percent air void criteria.

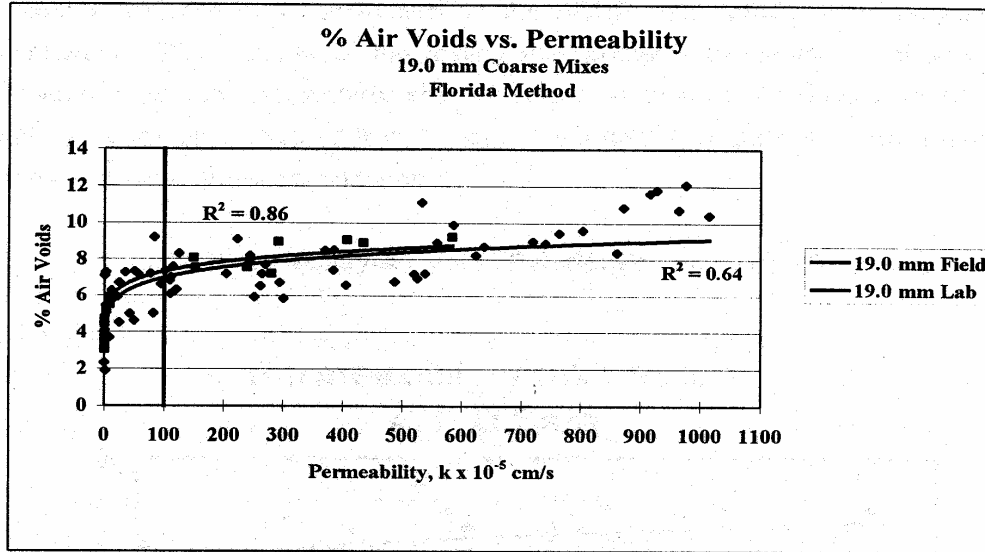


Figure 16. Florida DOT Permeability Test results. (15)

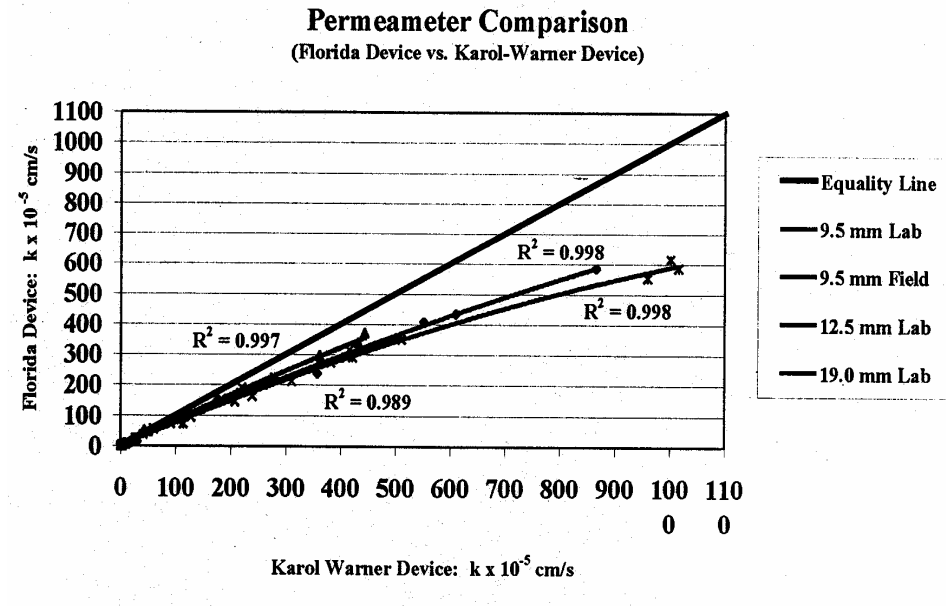


Figure 17. Comparison of the Karol-Warner and FDOT Permeameters. (15)

- 3) *Construction requirements:* Based on target permeability, Superpave construction specifications require a minimum in-place density of 94% of maximum density for coarse-graded mixtures (gradations passing below the Superpave restricted zone); and a

minimum in-place density of 92% of maximum for fine-graded mixtures (gradation curves passing above the Superpave restricted zone). In addition, the minimum lift thickness for coarse mixtures was increased to 3 times the maximum aggregate size of the mix. This requirement was in response to reports of difficulty in obtaining required field densities.

- 4) *Design requirements:* During mixture design, the minimum tensile strength ratio (TSR) as defined in AASHTO T-283 (the recommended Superpave moisture damage test for bituminous mixtures) was increased from 80% to 85%. This requirement is in anticipation of increased moisture exposure to field mixes, and hopes to give mixes an increased chance of withstanding that exposure.

Arkansas State Highway and Transportation Department Initial Studies

AHTD performed a number of permeability tests on field cores using a device originally designed and constructed for the ACHM permeability study previously mentioned. The purpose of the testing was primarily to identify a relationship between laboratory permeability and air voids. A total of 47 Superpave ACHM surface specimens, sampled from 16 jobs, were tested.

Figure 18 shows a plot of measured air voids versus permeability.

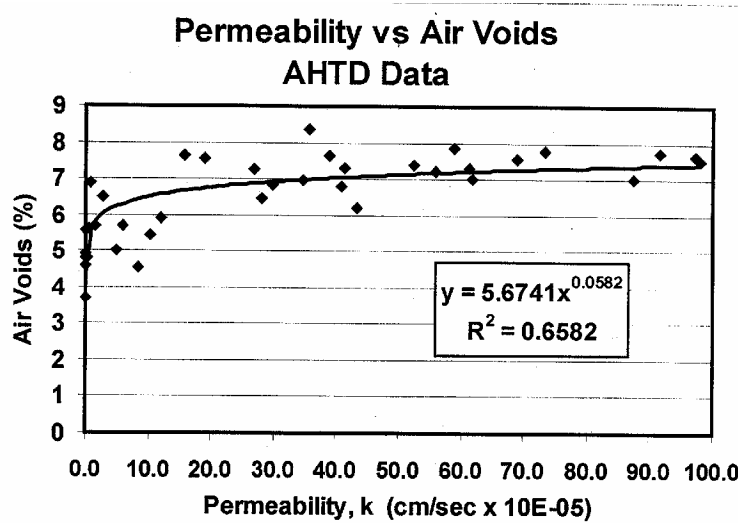


Figure 18. AHTD Permeability Study Results

Figure 18 indicates that permeability is very low for the Arkansas mixes tested having air voids less than about 6 percent. Above 6 percent, the specimens exhibit relatively high, and widely variable, permeability values. The data seems to corroborate similar data from Florida in the sense that 6 percent air voids may be considered to be a type of “breakpoint” maximum value relative to permeability. The absolute magnitude of permeability values shown in Figure 18 was not of prime importance at the time the AHTD presented its results. This is so because testing considerations and the effect of permeability on pavement performance have not been firmly established to date. *(12)*

CHAPTER 3

RESEARCH APPROACH

Project Objectives

The primary objective of the research was to develop strategies for considering ACHM permeability during design and/or construction. A number of specific objectives to be met in this study are reiterated:

- 1) *Document potential pavement problems caused by excess moisture.*
- 2) *Develop routine testing protocols for determining the permeability of ACHM.*
- 3) *Establish relationships between ACHM permeability and mixture performance.*
- 4) *Develop specific methodologies for considering permeability in design and construction.*

Project Scope

The research effort was divided into two major phases. Phase I in turn was divided into two major tasks. The first task consisted of developing relationships (if any) between permeability and air voids. The second task consisted of efforts to correlate –without the use of the usual intermediary (air voids) - pavement permeability and performance. During Phase II, testing parameters were varied in order to develop the best possible apparatus and assembly for accurately determining permeability of asphalt mixtures. Sample preparation procedures and testing protocols were also outlined in an attempt to develop a standardized permeability test that can serve as basis for ACHM acceptance.

For Phase I, a total of thirty-nine field core samples were studied from four different field projects (Springdale 71B, HWY 286 Greenbrier, HWY 22 Dardanelle, and Mt. Home By-pass). Also, a total of twenty-six laboratory-produced samples from three additional projects were tested (Virginia Round Robin, HWY 45 Hartford, I-40 Morgan). Laboratory samples were

produced using the Superpave Gyratory Compactor (SGC). These sixty-five samples represented one of two different mixture nominal maximum aggregate sizes: 12.5 mm or 25.0 mm. All samples (field cores or SGC pills) were tested for both major purposes in this phase: developing a relationship between air voids and permeability; and developing a relationship between permeability and performance.

For Phase II, a total of eleven field core samples were studied from projects using mixes produced at three different asphalt production plants (Jenny Lind [Arkholá], Freshour, and Lowell). A total of thirty-four laboratory-produced samples (taken from the same projects as the field cores) were also tested. As in the case in Phase I, these samples represented one of two different mixture nominal maximum aggregate sizes: 12.5 mm and 25.0 mm.

For specific gradation, binder content, binder gradation, and other mix design characteristics please refer to the mix design information presented in Appendix A.

EXPERIMENTAL PROCEDURES

Phase I (Task I – Relationship between Permeability and Air Voids)

During the execution of this research, a recognized standard test for determining the hydraulic conductivity of asphalt mixtures did not exist; the method used to initially calculate permeability of HMAC samples was that provided by the ASTM Committee D-4 (subcommittee 4-23). The method developed as part of this research, however, formed the basis for the subsequent standard permeability test adopted by ASTM. Appendix B contains instructions (used in this research) that cover preparation of ACHM test specimens and permeability testing, including the calculation of permeability, using the Karol-Warner Flexible Wall Permeameter.

Phase I (Task II- Relationship Between Permeability and Performance)

After samples were tested for permeability, they were subjected to performance testing using ERSA (Evaluator of Rutting and Stripping in Asphalt), a Hamburg wheel tracking test machine. Appendix C contains a complete and detailed description of the preparation of the samples for ERSA testing and the ERSA test itself. Additional information regarding the development of ERSA and the use of wheel-tracking tests to estimate mixture performance is given by Williams. (17) It is important to note that the amount of time between execution of the permeability tests and the performance test was minimized as much as possible. The sealant preferred for the sample preparation for permeability testing (Vaseline) is petroleum based; after time, some of the asphalt binder may be separated from the aggregates close to the surface of the sample. This could accelerate the stripping process once the ERSA test has commenced, leading to an inaccurate estimate of performance behavior.

Phase II (Design of Testing Protocols)

The overall objective of this phase of the research involved the identification and refinement of a laboratory testing procedure that could be easily reproduced while providing consistent and accurate measurements of permeability. Another related objective was to check the validity (applicability) of Darcy's law in asphalt concrete samples. According to ASTM D 5084-90, the validity of Darcy's law may be evaluated by measuring the hydraulic conductivity of the specimen at three different hydraulic gradients. If all measured values are similar (within approximately 25%), then Darcy's law may be taken as valid.

The particular testing issues considered in this Phase included the type of permeability test, the saturation level reached during sample preparation, and the suggested height of the sample to be tested. Details related to each of these issues follow.

Test Type / Apparatus - The actual tests performed in this phase included two permeameter assemblies. All samples were tested in the falling head permeameter assembly. Most samples were also tested in the falling head/rising tail permeameter assembly. A description of both tests used in this Phase follows.

Falling Head Permeability Test

Permeability testing was performed generally in accordance with the descriptions contained in the “Experimental Procedures” section of this report. However, a few adjustments were made for the sake of simplicity and to minimize testing time during execution. These modifications were identified and applied in this Phase based on results of intensive testing and data analysis, described in the “Results” section of this report. Modifications included the following:

- 1) All permeability tests were performed using a 10 ± 1 psi confining pressure only. An increase of the confining pressure to 14 psi was deemed unnecessary.
- 2) No single test was allowed to proceed beyond 30 minutes. Statistical analysis proved that time extensive tests produce results that are not statistically different than shorter tests.
- 3) The number of times the permeability test was repeated was reduced to 4.

Falling Head/Rising Tail Permeability Test

The second type of permeability test that was investigated was the falling head/ rising tail test. The assembly is very similar to the one described in previous sections. However, special modifications to the permeameter were required. A second standpipe (graduated cylinder) was

connected to the outlet of the permeameter so that it could serve as the collector of the water that has flowed through the sample, i.e. the tail standpipe. A reservoir of distilled water was connected to both the outlet of the permeameter and the second standpipe (refer to Figures 18 and 19). Two valves are used to control water flow. One was located between the outlet of the sample being tested (bottom plate of the permeameter) and the tail standpipe, referred to as “valve 1”. The other one controls the flow of water from the reservoir of distilled water to the entire system and is located between the tail standpipe and the reservoir, referred to as “valve 2” (see Figure 19). The procedure followed during testing of the samples is as follows.

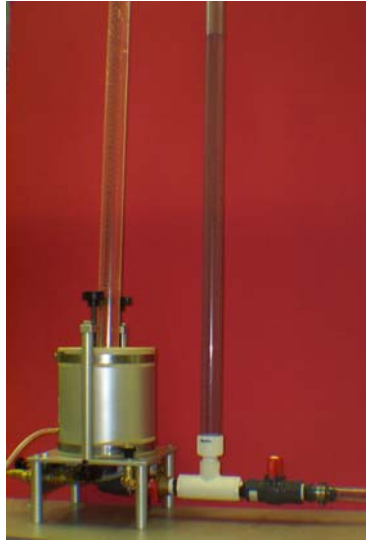


Figure 18. Falling head/ Rising Tail Test Permeameter Assembly.

Procedure

- 1) The samples tested under the procedure outlined in Phase II (falling head test), were tested in the falling head/rising tail permeameter assembly immediately after being removed from the unmodified-falling-head-test permeameter assembly. This is done to ensure that the sample loses a minimal percent saturation and that the detrimental effect of the Vaseline on the asphalt binder through time is reduced. However, since most of the

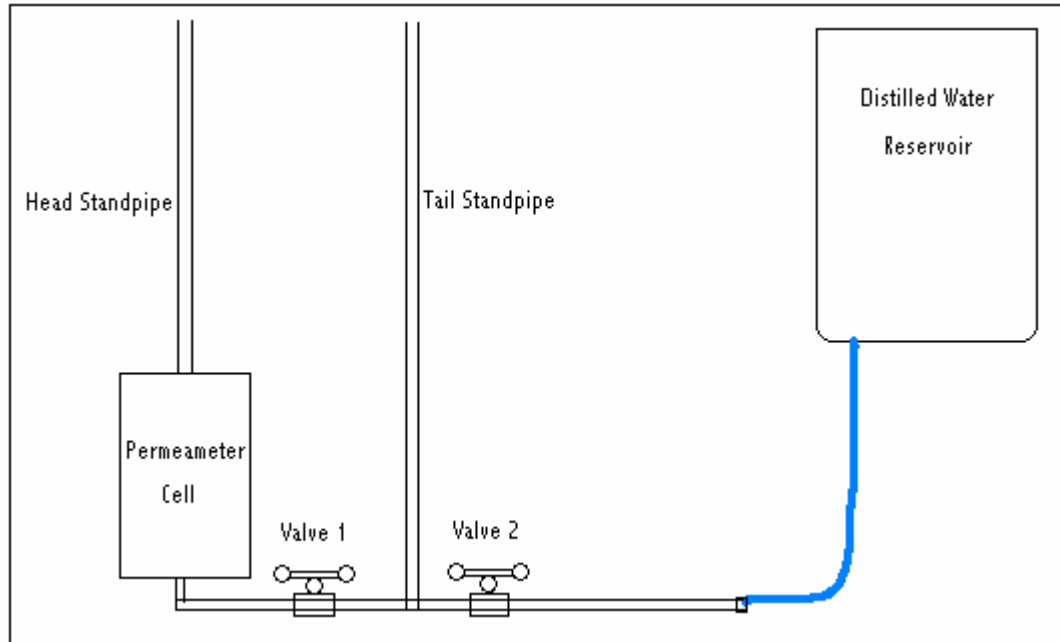


Figure 19. Schematic of the Falling Head/Rising Tail Test.

Vaseline that had initially covered the surface of the sample was probably removed during testing in the first permeameter assembly, a new Vaseline layer was added prior to placement in the second permeameter assembly.

- 2) After the permeameter has been assembled and tightened properly, a process of “back saturation” of the sample placed in the permeameter was performed. First, “valve 2” was opened allowing flow of water from the reservoir to the system. Water would fill the tail standpipe. Then, “valve 1” was opened, allowing water to flow from the tail standpipe to the sample. The flow rate of water from the tail standpipe, through the sample, and up into the head standpipe is related to the permeability of the sample. When the water level in the head standpipe was visible, i.e. the sample was entirely covered with water, “back saturation” was complete. “Valve 1” was then closed until tests were ready to commence.

- 3) Standpipes were marked for each individual sample. The marks were placed so as to satisfy the three hydraulic gradients studied in this research:

$$\Delta h = 2L, 5L, \text{ and } 8L$$

where

Δh – is the hydraulic gradient

L – is the length of each individual sample

The hydraulic gradients to be studied were achieved by marking the standpipes so that the net difference in elevation between the mark in the head standpipe (higher elevation) and the mark in the tail standpipe (lower elevation) is equal to the needed Δh . Required levels of water in both the head and tail standpipes (which are determined by the hydraulic gradient to be analyzed) were then reached by pouring water into the standpipes.

- 4) After water was poured into the standpipes and the levels at the standpipes reached the marks, the test was ready to be started. “Valve 1” was opened and the stopwatch was started. As water flowed from the head standpipe to the tail standpipe, the head loss (difference between the hydraulic heads at the head and tail standpipe) was recorded at given time intervals.

Calculation (both tests). During the falling head test, the SSD mass after vacuum saturation/soaking, sample dimensions, timing mark distances, and flow times were recorded. Calculation of the sample’s permeability was accomplished using Equation 12.

During the falling head/rising tail test, the hydraulic gradient, timing marks, and flow times were recorded. The SSD mass after vacuum saturation/soaking and the sample dimensions are the same as for the falling head test. Calculation of the sample’s permeability was done using

Equation 13. The area of the head standpipe, a_{in} , and the area of the tail standpipe, a_{out} , were found to be 9.7282 cm^2 and 6.4516 cm^2 , respectively, for use in Equation 13.

Report. For further analysis using data obtained from the falling head test, the permeability of the test specimen in units of 10^{-5} cm/sec , the height (thickness) of the specimen, the percent saturation, the soaking time, and the percent air voids to the nearest 0.1 percent were recorded.

For further analysis using data obtained from the falling head/rising tail test, the permeability of the test specimen in units of 10^{-5} cm/sec , the height (thickness) of the specimen, the percent saturation, the soaking time, the hydraulic gradient applied, and the percent air voids to the nearest 0.1 percent were recorded.

Preparation of Test Specimens. The procedure followed in this phase for sample preparation was similar to the one described in “Preparation of Test Specimens” in Phase I. However, several adjustments were required in this phase, detailed below.

- 1) Prior to vacuum saturation, a Void Pathway Test (VPT) was performed on the samples.

The VPT was developed to investigate the interconnectivity of the air voids in an ACHM sample and how this interconnectivity (rather than the air void content itself) affects the measured permeability of a sample. Ng describes the development and use of the VPT.

(18) This test proved effective when used for screening samples; samples that were deemed “impermeable” by the VPT were discarded rather than tested in the permeameter assemblies.

- 2) The specimen was allowed to soak in distilled water for periods of 10, 20, and 30 minutes after vacuum saturation to assure target saturation levels.

- 3) In order to observe the effect of the three different soaking periods on saturation levels, the saturated, surface dry (SSD) mass was obtained and compared to the SSD mass previously obtained according to AASHTO T 166.
- 4) The samples were sealed as soon as possible after determining its SSD mass. This was done in an attempt to prevent changes in the sample's saturation level before the permeability test was run.

Sampling

Loose Superpave mixes representing target nominal maximum aggregate sizes were sampled from asphalt plants within the state of Arkansas. In addition, some compacted samples were obtained from the Virginia Transportation Research Council, as part of an initial round robin investigation. Table 2 shows the locations from which loose mix was obtained and the corresponding number of samples produced with the Superpave Gyratory Compactor (SGC). Field cores were also obtained with close cooperation of the Arkansas State Highway and Transportation Department (AHTD) for permeability and performance tests. Table 3 shows the locations from which field pavement cores were obtained and the corresponding number of cores obtained from each location. It is noted that for Phase II all samples were pre-screened using the Void Pathway Test. Based on VPT results, many of the samples were eliminated and are not included in Tables 2 and 3.

Test samples had one of two nominal maximum aggregate sizes: 12.5 mm and 25 mm. For Phase I, laboratory samples were compacted between 4.9% and 7.8% voids, achieved by varying the number of gyrations in the gyratory compactor. Field cores for Phase I varied between 2.3% and 12.1% air voids. For Phase II SGC samples were compacted to a target 7.0% air voids. However, field core air void contents were beyond the researcher's control.

Location	Number of Samples
Virginia (Round Robin)	8
Highway 45, Hartford	12
Interstate 40 (I-40) Morgan	6
Jenny Lind Arkhola	13
Lowell	9
Freshour, Cabot	12
Total	60

Table 2. Location and number of SGC samples used for testing.

Location	Number of Samples
Springdale 71B	8
Highway 286, Greenbrier	2
Highway 22, Dardanelle	6
Mt. Home By-pass	23
Freshour, Cabot (I-40)	4
Jenny Lind Arkhola (US 71)	4
Lowell	3
Totals	50

Table 3. Location and number of Field Cores used for testing.

CHAPTER 4

TEST RESULTS AND DISCUSSION

Phase I (Task I - Relationship Between Air Voids and Permeability)

Data from a total of 110 ACHM samples was used for the development of a model that could be used to predict HMA permeability given percent air voids. Test specimens were categorized according to nominal maximum aggregate size (12.5 mm or 25 mm) and type of sample (field core or Superpave gyratory compacted sample). Figure 20 depicts the relationship between hydraulic conductivity (k) and percent air voids for all samples tested. While a general trend is evident, a “best fit” power curve representing the relationship does not provide a suitable predictive equation (as evidenced by the low R^2 value). However, Figure 20 generally corroborates the conclusions offered by numerous researchers, namely, that hydraulic conductivity drops to very low levels when air voids drop below six percent.

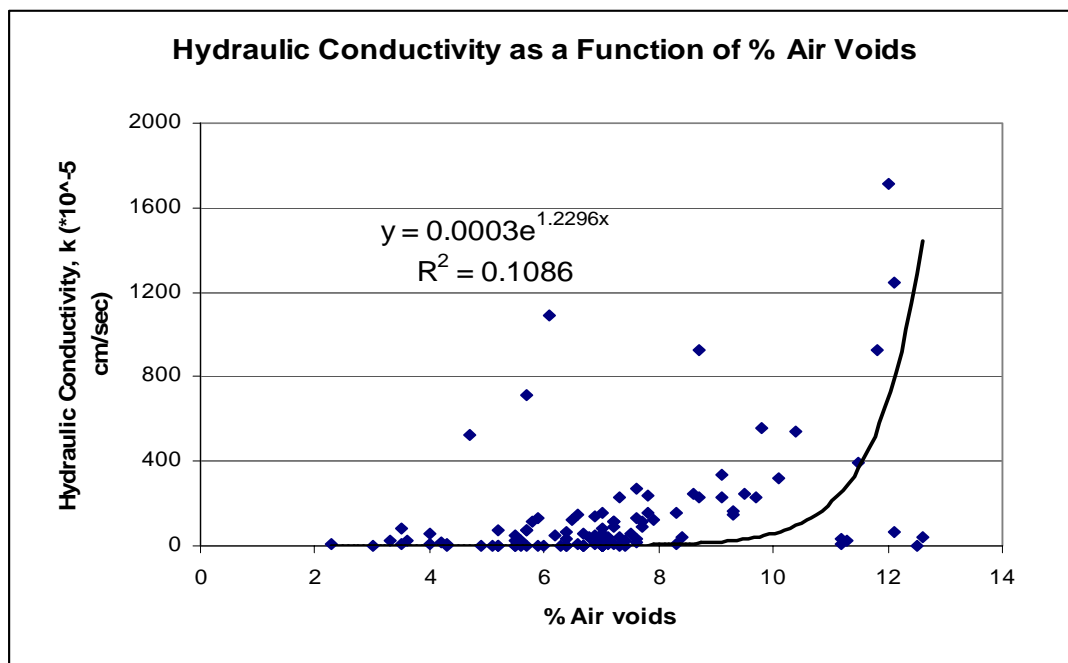


Figure 20. Relationship Between Air Voids and Permeability – All Samples

In addition to the general relationship shown in Figure 20, permeability versus air voids data was analyzed for various subgroupings, e.g. nominal maximum aggregate size and field versus lab-compacted cores. Combinations of the subgroupings were also evaluated. Table 4 summarizes the subgroupings considered and corresponding R^2 values for the best-fit relationships. It is evident from Table 4 that a power-function based equation does not adequately describe the relationship between permeability and air voids for this particular set of samples.

Sample Grouping	R^2
All samples	0.1086
12.5 mm mix (all samples)	0.3223
25 mm mix (all samples)	0.2858
Lab-compacted samples (all NMAS)	0.2708
Field cores (all NMAS)	0.2036
Laboratory-compacted samples / 12.5 mm	0.3105
Laboratory-compacted samples / 25 mm	0.6030
Field cores / 12.5 mm	0.3248
Field cores / 25 mm	0.0248

Table 4. Summary of Permeability versus Air Voids Models

The final step in this phase was to consider the possibility that the relationship between permeability and air voids is mix-specific. Should this prove true, the creation of a model for predicting permeability of asphalt mixtures becomes impractical. Three projects were used for this evaluation: Springdale 71B (a 12.5 mm mix), Mt. Home By-Pass (a 25 mm mix), and AR 45 Hartford (a 12.5 mm mix). In general, project-specific air voids / permeability relationships were better (higher R^2 values) than those generated for the large data sets.

Phase I (Task II - Relationship Between Permeability and Performance)

For this research, the total deflection (rut depth) of samples after 20,000 cycles (wheel passes) of the Evaluator of Rutting and Stripping of Asphalt (ERSA) was used as the measure of pavement performance. Figure 21 is an example of an ERSA result. A typical sample will experience some initial consolidation, then deform at a rate known as the rutting slope. The rutting slope is defined as the slope of the deformation curve, as measured in the linear portion of the curve. Then if the sample strips, the slope of the deformation curve will increase. The linear portion in this region is known as the stripping slope.

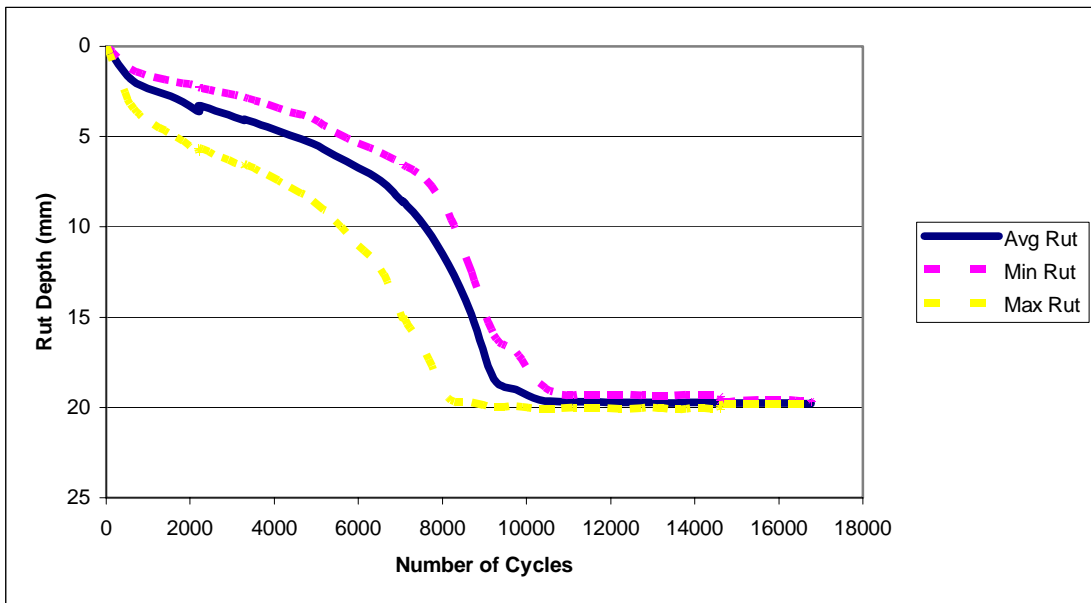


Figure 21. Typical ERSA Output.

Figures 22-24 show ERSA outputs of samples with different magnitudes of hydraulic conductivity. Figure 22 depicts results from 12.5 mm specimens. Inconsistencies in performance are noted. Samples with hydraulic conductivity values as high as 240×10^{-5} cm/sec do not strip at all, while virtually impermeable samples (k value of only 1.2×10^{-5} cm/sec)

stripped at 10,000 cycles. Furthermore, the samples that exhibited the largest total rut depth were in fact, the ones with lowest hydraulic conductivity.

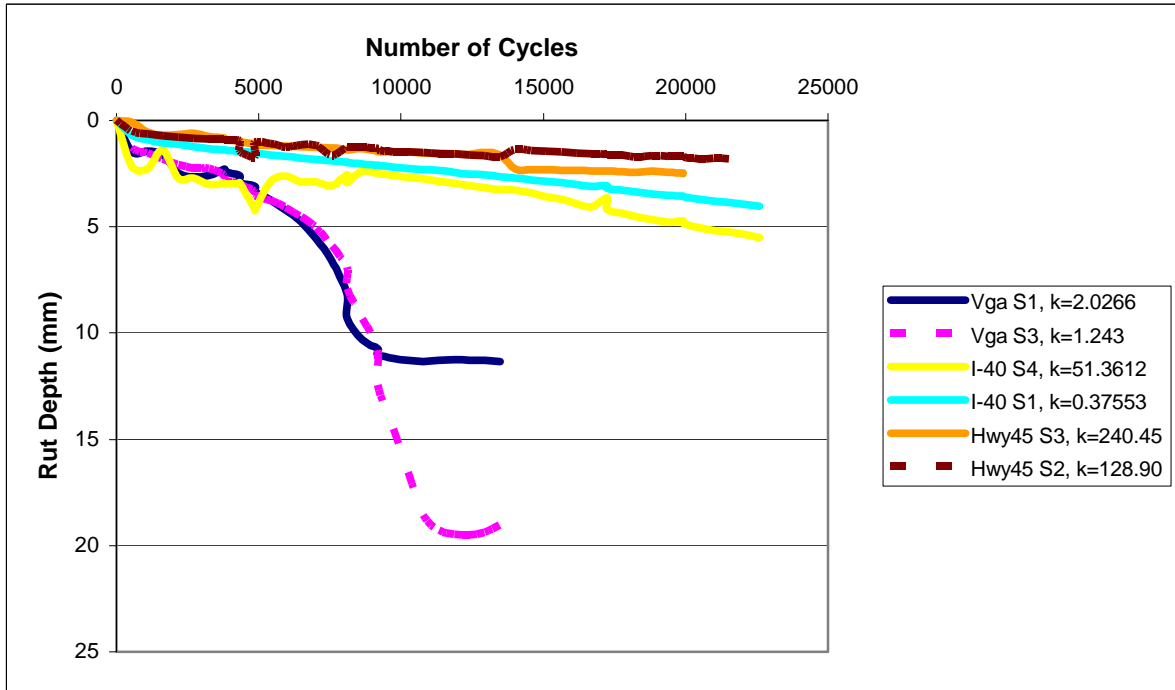


Figure 22. ERSA Results: 12.5 mm Laboratory Samples

Figure 23 shows selected ERSA results representing field cores from 12.5 mm nominal maximum aggregate size mixtures. As with the results shown in Figure 22, the results in Figure 23 exhibit inconsistencies in the expected relationship between permeability and wheel-tracking results. For example, sample 9a from Mt. Home (impermeable: k value of 0×10^{-5} cm/sec), rutted and stripped rather excessively. Conversely, sample 12 from Highway 286 exhibited a relatively large k value (4713.58×10^{-5} cm/sec), but performed better.

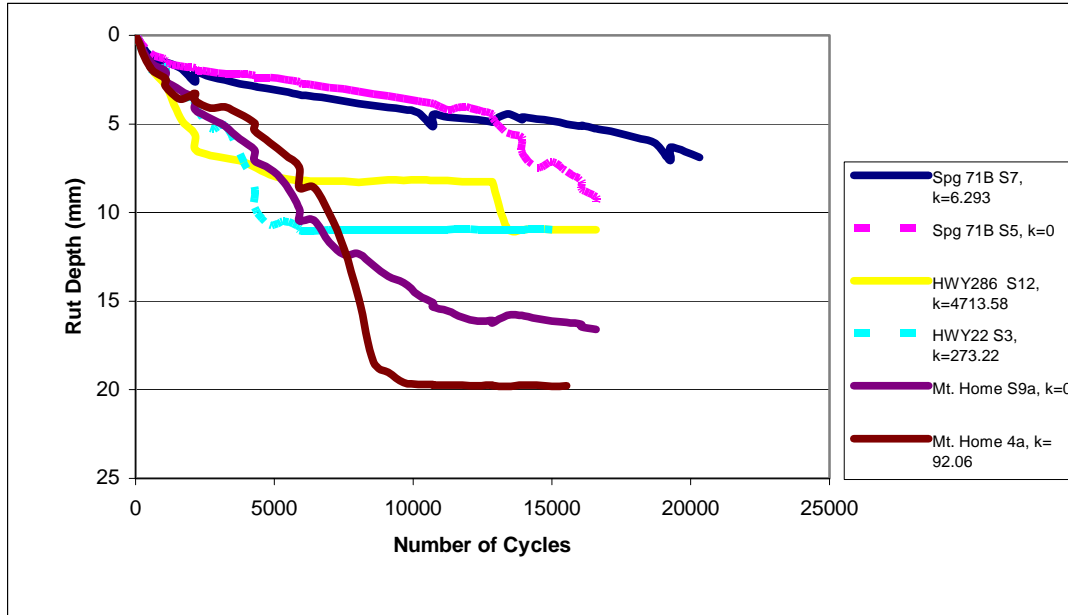


Figure 23. ERSA Results: 12.5mm Field Cores

Figure 24 shows ERSA results for field cores taken from mixtures with 25 mm nominal maximum aggregate size. Within this small data set, the ‘expected’ pattern (increased permeability yielding lower performance) is more pronounced. For example, sample 3b (relatively large k value of 4882.66×10^{-5} cm/sec) performed very poorly. The other three samples shown all exhibited relatively low permeability values and relatively good performance.

A general conclusion reasonably drawn from the ERSA results generated in this research is that an ACHM sample exhibiting high permeability value tends to perform poorly in terms of rutting and stripping behavior. However, the opposite is not always true; that is, samples with low permeability values do not necessarily perform well – many also perform poorly. It is noted that many factors contribute to the rutting and stripping performance of hot-mix asphalt concrete. The fact that permeability, as a single factor, is not a one hundred percent reliable predictor of rutting/stripping performance is not surprising nor necessarily significant.

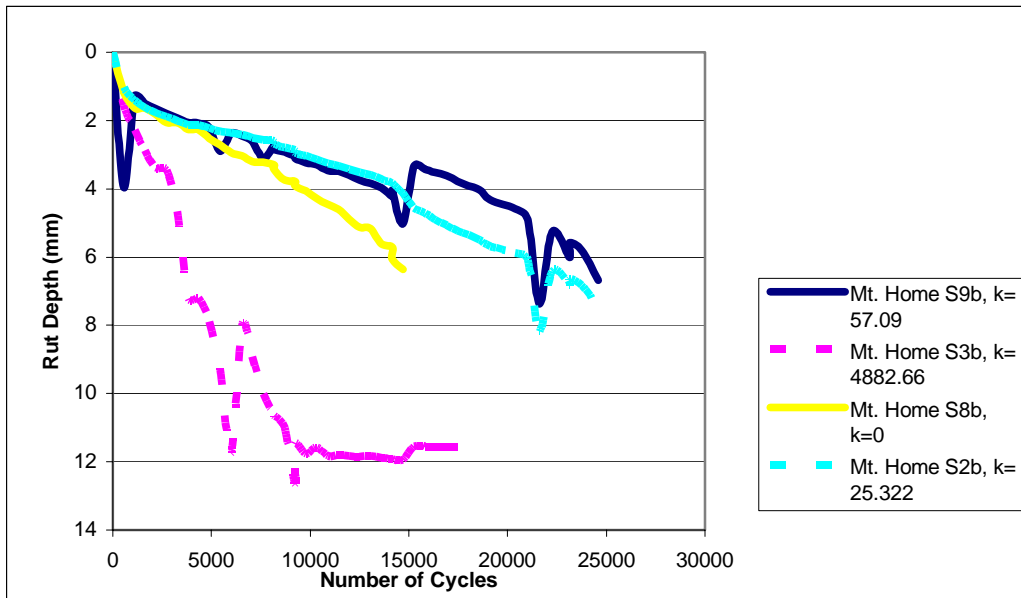


Figure 24. ERSA Results: 25 mm Field Cores

Data from ERSA testing was used to evaluate relationships between permeability and total rut depth at 20,000 wheel passes. Results were subdivided according to specimen type (field versus lab). Only mixtures with 12.5 mm nominal maximum aggregate size were evaluated; there was insufficient data for mixtures with 25 mm nominal maximum aggregate size to make meaningful comparisons.

Figures 25-27 show the relationship between permeability and rut depth at 20,000 wheel passes. The relatively flat curve represented in each of Figures 25 through 27 suggests that no consistent, significant relationship was discovered in this research.

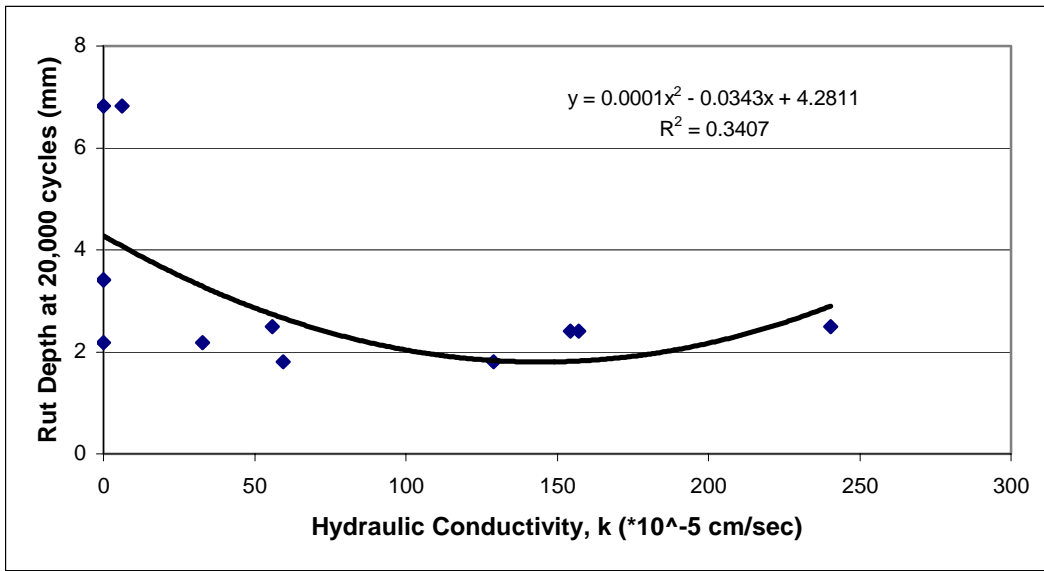


Figure 25. Relationship Between ERSA Rut Depth and Permeability, 12.5 mm Laboratory Samples

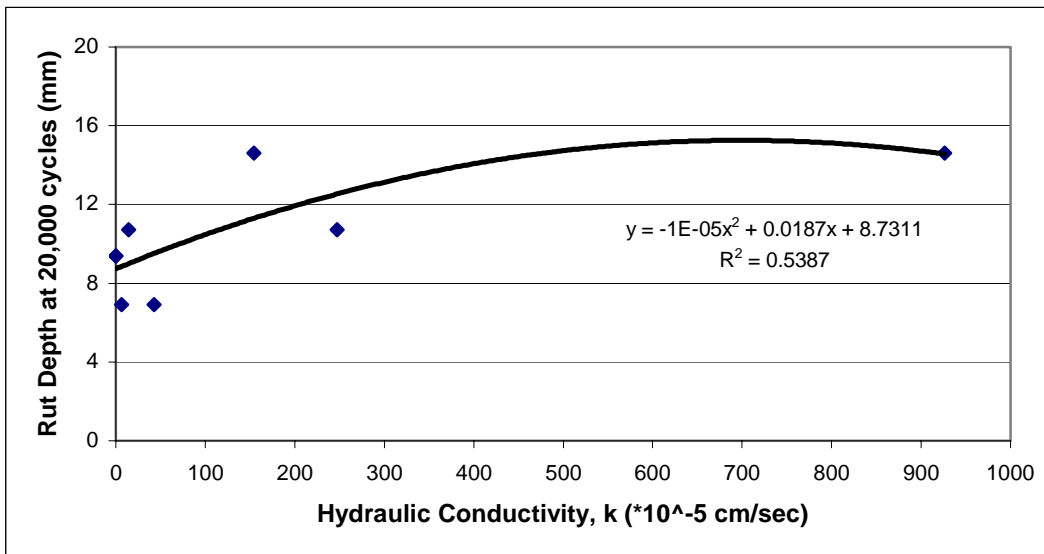


Figure 26. Relationship Between ERSA Rut Depth and Permeability, 12.5 mm Field Cores (Hartford AR 45)

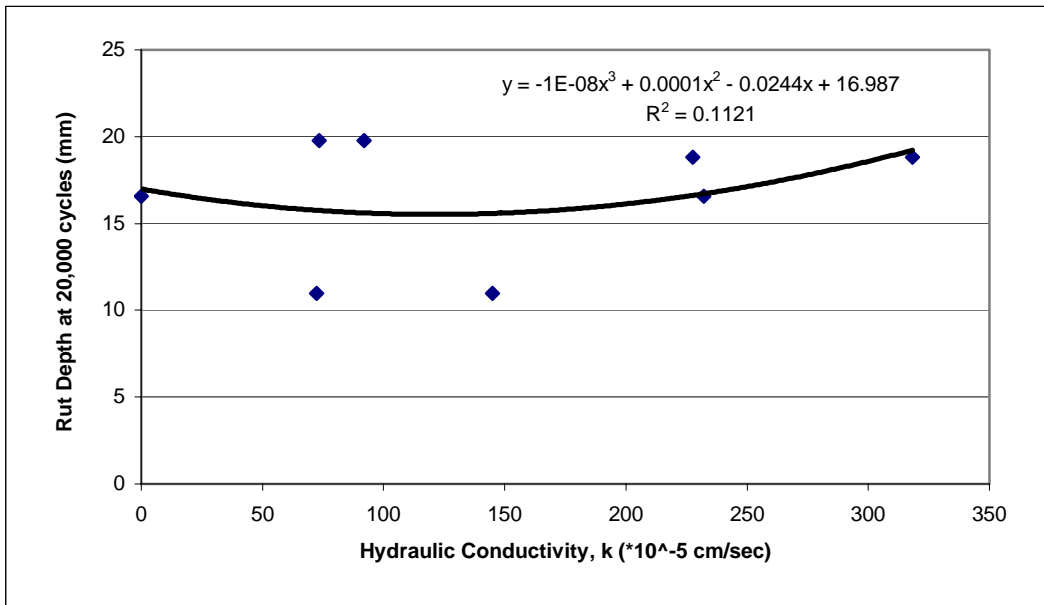


Figure 27. Relationship Between ERSA Rut Depth and Permeability, 12.5 mm Field Cores (Mt. Home By-Pass)

Phase II (Test Protocol Refinement)

The primary objectives of Phase I were associated with the development of relationships between air void content, permeability, and ACHM performance; however, testing protocols were also addressed. Some initial modifications to testing procedures were made prior to the full investigations comprising Phase II of this project. These modifications were based on the results, observations, and analyses performed during Phase I. For clarity, these investigations, while not technically performed during “Phase II”, are included here in order to group all testing protocol related information.

As stated in Chapter 3 (Experimental Procedures), each sample was tested using two confining pressures, 10 and 14 psi. Readings of the head loss were taken at different time intervals until the entire 63.51 cm of head (equivalent to 500 mL of distilled water) flowed

across the sample, regardless of the elapsed time for a complete test. These two considerations – double confining pressure and full-flow time recording – led to time consuming tests (in some cases exceeding ten hours per sample). In addition, the water that flowed through the sample was collected in a pan and weighed, to ensure that sample saturation was not decreasing as the test was performed. These procedures were evaluated with a target of reducing, if warranted, total testing time.

Confining Pressure

The initial version of the permeability test required the operator to run five tests using a 10 psi confining pressure, then repeating five tests using 14 psi pressure. The results obtained were analyzed to investigate if confining pressure had an effect on hydraulic conductivity values calculated from the tests. Specifically, results obtained under 10 and a 14 psi confining pressure were evaluated to determine if such results were statistically different. Two sets of samples were studied: Virginia Round Robin and HWY286/HWY22/Springdale71B. Samples from the first group are laboratory (gyratory-compacted) samples. Samples from the second group are field cores. An Analysis of Variance (ANOVA) test was performed on both data sets. Table 5 illustrates that confining pressure had no effect on calculated permeability.

ANOVA Test	F_{critical}	F_{actual}	Conclusion
1) Gyratory	4.46	1.1550059	Confining Pressure has no effect on measured k
2) Field Cores	4.46	0.25121999	Confining Pressure has no effect on measured k

Table 5. ANOVA Results for Confining Pressure Evaluation

Since the ANOVA tests showed that there is no statistical difference between the hydraulic conductivity values obtained at 10 psi and 14 psi confining pressure, all tests in Phase II were done at only one confining pressure – 10 psi. Factors considered in the selection of 10 psi confining pressure included:

- 1) Variability within the 5 tests performed at 10 psi confining pressure was lower than the variability for test results obtained at 14 psi confining pressure.
- 2) A 14 psi confining pressure may be excessive. When this pressure was applied to the confining membrane, the sealant (Vaseline) is squeezed from the voids on the side surface onto the top surface and into the inner voids of the sample, influencing the flow of water – potentially affecting calculated permeability value.

Time of Reading

The initial test protocol required the operator to take readings of the head loss at different time intervals until the entire head (500 mL of distilled water) flowed through the sample. However, some of the samples had so low a permeability that this required more than one hour. Tests on such samples were stopped after one hour, with readings taken at 15, 30, 45, and 60 minutes. Permeability results calculated using the readings taken at each time interval were evaluated using an analysis of variance (ANOVA), in order to determine if the time of reading (or the duration) of the test had a significant influence on the results. Table 6 shows the results for the ANOVA. Note that the analysis was performed using data corresponding to both 10 and 14 psi confining pressure. This was done since, at the time, pressure had not been excluded as a non-determining factor in permeability testing. As seen in the Table 6, time of reading did not affect the value of permeability calculated for the samples tested in Phase I.

ANOVA Test	F_{critical}	F_{actual}	Conclusion
1) Samples tested at 10 psi	3.84	0.001052	Time of reading has no effect on measured k
2) Samples tested at 14 psi	3.84	0.01420531	Time of reading has no effect on measured k

Table 6. ANOVA Results for Testing Time Evaluation

Since no statistical difference between the hydraulic conductivity values obtained from the various time intervals was noted, it was concluded that time interval should be user-defined. In this sense, and in an attempt to reduce the duration of the tests, no single reading was taken beyond 30 minutes in tests performed during Phase II. However, in order to ensure consistency, at least 3 readings were taken during each test. Every sample was still subjected to 4 tests (enough to yield a meaningful standard deviation) with a 10 psi confining pressure.

Figure 28 illustrates the insignificance of test time on the calculated permeability; the results shown in Figure 28 are typical of all results generated. Generally, points plot in the same horizontal band (signifying a relatively constant permeability) regardless of the time of reading. Close inspection of Figure 28 uncovers another important aspect in permeability testing: the effect of sample saturation. The four lowermost points plotted in Figure 28 all belong to the first test at a 10 psi confining pressure, i.e. they were the first four readings to be taken on this sample. These readings not only yielded low permeability values, but also showed a gradual increase in the sample's permeability. After these four readings were taken, however, all points plotted in a relatively constant permeability range. It is hypothesized that the sample had not been properly saturated, and that the first test (which delivered 500 mL of water through the sample) effectively saturated the sample.

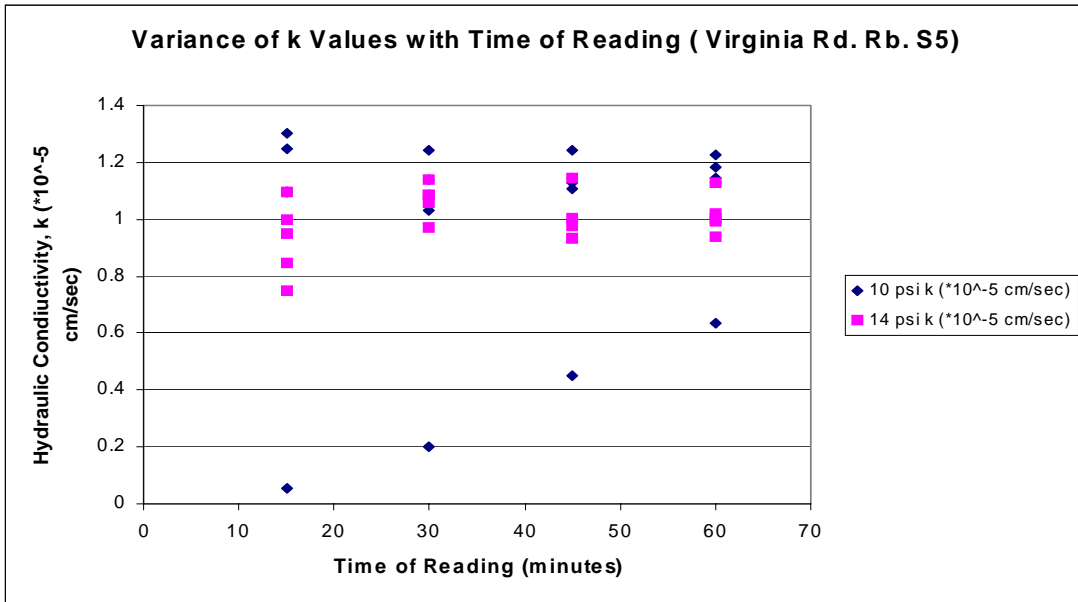


Figure 28. Relationship of Permeability to Testing Time (typical)

Water Collection and Measurement

In Phase I, water was collected in a pan and weighed, in accordance with initial testing protocols. Table 7 shows the mass of the water collected for select Phase I tests. Ideally, the pan should collect approximately 500 grams of water if 500 mL of water flowed through the sample being tested. Table 7 shows that the largest amount of water collected was 518.4 grams. However, it is likely that this deviation can be attributed to the difficulty inherent in closing the valve that essentially “stops” a falling head test. Based on the data shown in Table 7 and the aforementioned difficulties associated with closing the valve in a consistent manner, this procedure was omitted from the testing sequence employed in Phase II.

Sample	Test 1 gms	Test 2 gms	Test 3 gms	Test 4 gms	Test 5 gms
1	507.5	508.2	508.0	504.8	508.7
2	504.3	509.5	511.5	512.5	512.9
3	498.0	509.9	510.1	510.8	512.0
4	518.4	518.0	504.2	513.7	507.2
5	489.1	505.7	508.5	507.9	512.8
6	509.3	513.2	509.8	513.3	508.1
7	491.7	513.8	504.5	513.2	508.0
8	514.2	508.2	509.9	513.7	510.5

Table 7. Water Collected for Phase I Falling Head Tests

Phase II (Refinement of Testing Protocols) -- Continued

Data from a total of 45 samples was used for investigating the effect of initial hydraulic gradient, test specimen height, and the level of saturation on calculated permeability. In addition, an additional investigation was performed to evaluate the effect of a “pre-soaking” period on the saturation level of ACHM test specimens. As in Phase I, samples were categorized according to their nominal maximum aggregate size, type of compaction, and site.

Hydraulic Gradient

A falling head / rising tail permeability test was employed to investigate the effect of initial hydraulic gradient on calculated permeability. The initial hydraulic gradient was defined as the difference between the water levels in the head standpipe and the tail standpipe of the permeameter assembly. Three different hydraulic gradients were evaluated for each individual sample: 8L, 5L, and 2L, where L is the length (height) of each individual sample. As mentioned

in Chapter 2, Darcy’s Law is considered to be valid if the permeability values calculated using all three hydraulic gradients are within 25 percent. For this investigation, three sample sets were used:

- 1) Jenny Lind Arkhola: 12.5 mm, laboratory-compacted (10 samples).
- 2) Freshour, Cabot: 12.5 mm, laboratory-compacted (6 samples).
- 3) Lowell: 25 mm, laboratory compacted (6 samples).

Table 8 shows the results obtained from the ANOVA performed using the permeability results for the samples shown above.

Sample Set	F_{critical}	F_{actual}	Significant Effect?
Jenny Lind Ark.	3.71	7.342	Yes
Freshour Cabot	4.76	4.969	Yes
Lowell	4.76	0.4708	No

Table 8. ANOVA Results for Initial Hydraulic Gradient Evaluation

The mixed results shown in Table 8 do not definitively establish the significance of the initial hydraulic gradient. However, measured permeability values must be within 25 percent in order for Darcy’s Law to be valid (implying that hydraulic gradient has no effect on measured permeability) – thus, another analysis may be made. Table 9 shows a comparison of permeability values obtained using various hydraulic gradients. The “percent difference” shown in Table 9 is normalized to the permeability calculated from the data obtained using the “2L” gradient.

Sample #	k@2L	k@5L	%Difference	k@8L	%Difference
Lowell 1	11.151	22.154	50.33	31.42	70.51
Lowell 2	32.758	50.164	65.30	73.522	68.23
Lowell 3	1.103	2.469	44.67	4.813	51.30
Lowell 4	102.598	185.543	55.30	283.19	65.52
Lowell 5	10.979	20.408	53.79	26.38	77.36
Freshour 1	14.252	28.486	50.03	40.263	70.750
Freshour 2	19.036	40.429	47.09	58.67	68.91
Freshour 3	19.725	37.141	53.11	56.425	65.82
Freshour 4	22.589	47.867	47.19	97.548	49.07
Freshour 5	11.417	33.698	33.88	68.511	49.186
JennyLind 1	13.17	25.441	51.767	34.393	73.88
JennyLind 2	8.244	12.386	66.56	14.919	83.02
JennyLind 3	15.196	36.465	41.67	50.761	71.84
JennyLind 4	19.614	37.016	52.99	50.647	73.086
JennyLind 5	14.418	28.852	49.97	39.696	72.68
JennyLind 6	17.733	41.644	42.58	60.153	69.23
JennyLind 7	7.578	14.93	50.757	20.623	72.39
JennyLind 8	18.306	42.048	43.53	62.371	67.42
JennyLind 9	15.675	32.964	47.55	49.674	66.36

All permeability values shown expressed as cm/sec x 10⁻⁵

Table 9. Effect of Initial Hydraulic Gradient on Permeability

Only one set of permeability values of the nineteen cases shown in Table 9 meets the “25%” rule regarding the validity of Darcy’s Law. In this sense, it may be concluded that the initial hydraulic gradient did affect the measured hydraulic conductivity and, therefore, Darcy’s Law is not valid. This conclusion challenges the accuracy of permeability testing for ACHM using the current procedures.

Sample Height

Laboratory samples using mix from Lowell, Jenny Lind, and Cabot were compacted to two heights, approximately 70 mm and approximately 90 mm. With use of the Void Pathway Test (VPT) (*18*) it was observed that more than 85 percent of samples compacted to a height of 90 mm were impermeable. One possible explanation for this observation is that interconnected voids do not traverse completely through (top to bottom) a tall sample, but rather branch off to the sides of the specimen. For this reason, only samples smaller than 70-75 mm in height were tested.

Effect of Sample Soaking on Percent Saturation

Literature related to permeability testing, as well as data from this research project, shows that percent saturation affects the hydraulic conductivity measured for an ACHM sample. Generally, the closer the sample is to being 100% saturated, the more accurate the measured value of permeability should be. Thus, saturation procedures must be evaluated. During this project, all samples were saturated by means of a vacuum pump. In Phase I, samples were subjected to a 28 mm of Hg vacuum while submerged in water for 15 minutes followed by a period of soaking that lasted 5 to 10 minutes. To study the possible effect of soaking time on percent saturation, samples tested in Phase II were vacuum saturated in the same manner, but they would then soaked for periods of 10, 20, or 30 minutes. Percent saturation was recorded

after soaking. Figure 29 shows a plot of percent saturation vs. time of soaking. The results shown in Figure 29 suggest that various soaking times did not have a significant effect on the resulting degree of saturation for the ACHM specimens.

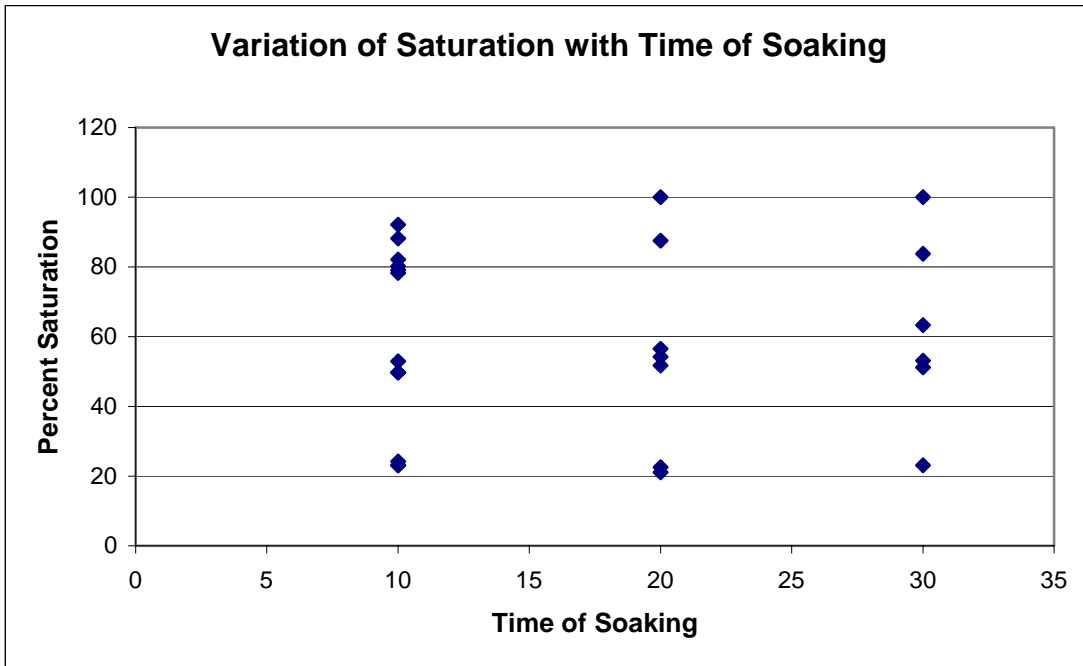


Figure 29. Effect of Soaking Period on Degree of Saturation

Percent Saturation

As previously stated, hydraulic conductivity as defined using Darcy's Law is valid only if the sample is fully saturated. Statistical analysis could not be performed on the data obtained for examination of this issue; in order to do so, replicate tests would need to be performed at various saturation levels. This is not possible for a single specimen – a specimen is coated with sealant upon use, and “re-saturation” is not possible. For this reason, alternative methods (other than strict statistical analysis) were used to interpret the data obtained.

One method used to evaluate the effect of saturation level on permeability is to examine a plot of the data. However, this type of evaluation must consider the air void content of the test specimen. Accordingly, samples were categorized into three groups according to their percent air voids. These groups were:

- 1) Samples with percent air voids less than, and including 7.0 %
- 2) Samples with percent air voids between 7.0% and 9.5%
- 3) Samples with more than 9.5%

Figures 30 through 32 show the relationship between percent saturation and hydraulic conductivity, for the respective air void categories noted above. No apparent pattern is readily noticeable from these figures – however, it is suggested that ACHM samples for permeability testing purposes should always be vacuum saturated and soaked if possible.

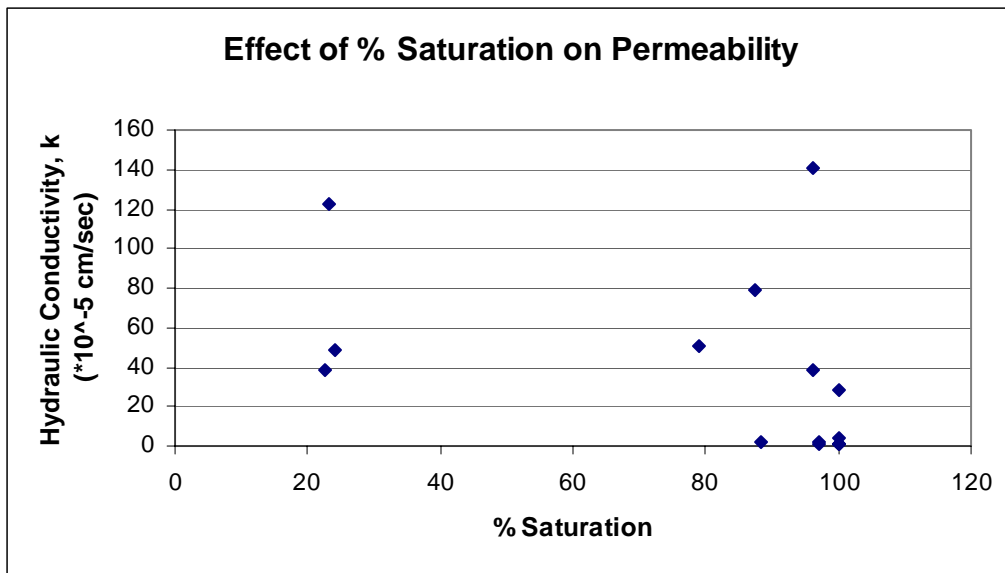


Figure 30. Effect of Saturation on Hydraulic Conductivity – Low Voids

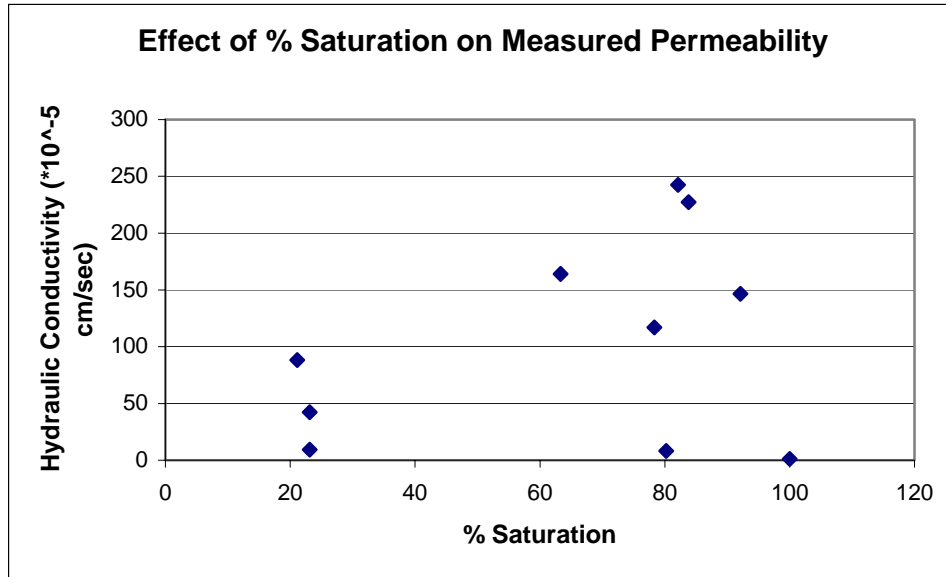


Figure 31. Effect of Saturation on Hydraulic Conductivity – Medium Voids

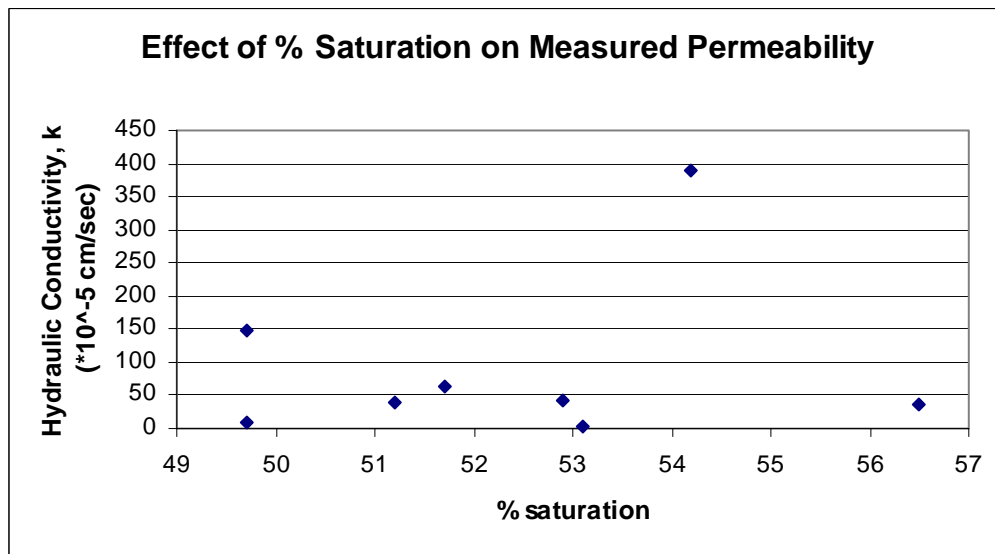


Figure 32. Effect of Saturation on Hydraulic Conductivity – High Voids

CHAPTER 5

CONCLUSIONS AND RECOMMENDATIONS

In general, project objectives were addressed. Chapter 2 documents the development of ACHM permeability concepts and potential pavement problems caused by excess moisture. Chapters 3 and 4 document efforts to develop routine testing protocols for measuring the permeability of ACHM. Chapters 3 and 4 also document attempts to relate ACHM permeability to rutting/stripping performance as estimated by the ERSA loaded-wheel tester. However, due to the inability to develop consistent models for estimating permeability using ACHM mixture properties, and the inability to establish a consistent relationship between permeability and performance, specific methodologies for considering permeability in ACHM mixture design and construction were not identified.

Results presented in this report are not enough to justify modification of current Superpave mix design procedures. Although a permeability test that could be considered a standard test was developed, it is suggested that it be refined and perfected with additional testing and statistical analysis.

Based on the data presented in this report, the following conclusions and recommendations are offered:

- 1) Permeability of ACHM seems to increase significantly when specimens have air voids in excess of six to seven percent.
- 2) A robust mathematical relationship between permeability and air voids appears to be mixture-specific; contributing factors include nominal maximum aggregate size and compaction method.

- 3) ACHM permeability does not exhibit a consistent relationship to performance as measured by laboratory wheel tracking.
 - a) Wheel-tracking performance seems to be more closely related to compactive effort (air void content) and mixture characteristics such as aggregate structure and gradation.
 - b) While not all ACHM specimens with low permeability performed well, ACHM specimens with relatively high permeability generally performed poorly in wheel tracking tests.
- 4) A standard permeability test for ACHM may be performed using falling-head methods, subject to the following constraints:
 - a) A single confining pressure of 10 ± 1 psi may be used.
 - b) The duration of the test and the time at which readings are taken may be user-defined.
 - c) A single sample must be tested at least 3 times in order to obtain a value for standard deviation.
 - d) Before any reading is taken, a full 500 milliliters of water should be let to flow through the sample to ensure sufficient sample saturation.
 - e) Samples should not exceed 75 mm in height.
- 5) Initial hydraulic gradient affects measured hydraulic conductivity.
 - a) Darcys' Law may not be valid for falling-head measurement methods used in conjunction with ACHM samples.
 - b) This issue should be further investigated if advances are to be made on permeability testing of asphalt mixtures.

- 6) Special care should be given to sample saturation.
 - a) To ensure full saturation, samples to be tested should be vacuum-saturated for 15 \pm 2 minutes and soaked in water as long as is practical.

REFERENCES

1. Carpenter, S. H., Darter, M. I., and Dempsey, B. J., “A Pavement Moisture-Accelerated Distress (MAD) Identification System, Volume I”, FHWA/RD-81/079, Federal Highway Administration, September 1981.
2. Scheidegger, F. L., Flow Through Porous Media, First Edition, McGraw-Hill, San Francisco, California, 1963.
3. Das, B. M., Principles of Geotechnical Engineering, Fourth Edition, PWS Publishing Company, Boston, MA, 1998.
4. Leonards, G. A., Foundation Engineering, McGraw-Hill, New York, 1962.
5. Tan, S. A., Fwa, T. F., and Chuai, C. T., “A New Apparatus for Measuring the Drainage Properties of Porous Asphalt Mixtures”, Journal of Testing and Evaluation, JTEVA, vol. 25, No. 4, July 1997.
6. Tan, S. A., Fwa, T. F., and Chuai, C. T., “Automatic Field Permeameter for Drainage Properties of Porous Asphalt Mixes”, Journal of Testing and Evaluation, JTEVA, vol. 27, No. 1, January 1999.
7. American Society for Testing and Materials, “Standard Test Method for Measurement of Hydraulic Conductivity of Saturated Porous Materials Using a Flexible Wall Permeameter” ASTM D 5084-90, Philadelphia, PA, 1997.
8. McLaughlin, J. F. and Goetz, W. h., “Permeability, Void, Content, and Durability of Bituminous Concrete”, Proceedings, Highway Research Board, Vol. 34, 1955.
9. Hein, T. C., and Schmidt, R. J., “Air Permeability of Asphalt Concrete”, ASTM Special Publication No.309, 1961.

10. Shklarsky, E., and Kimchi, A., “Influence of Voids, Bitumen and Filler Content on Permeability of Sand-Asphalt Mixtures”, Bulltein 358, Highway Research Board, 1962.
11. McWilliams, C. E., “Air and Water Permeability Related to Asphalt Mix Characteristics”, MS Thesis, University of Arkansas, Fayetteville, AR, 1986.
12. Hall, K. D., “ Permeability of Superpave”, Interim Report, University of Arkansas, Fayetteville, AR, 1999.
13. Zube (1960s)
14. Brown, Collins, and Brownfield (1989)
15. Choubane, B., Page, G., and Musselman, J., “Investigation of Water Permeability of Coarse Graded Superpave Pavements”, Research Report FL/DOT/SMO/97-416, Florida Dept. of Transportation, Gainesville, Florida, July 1997.
16. Musselmen, J., “Florida’s Experience with Superpave and Permeability”, presentation given to the Southeastern Asphalt User-Producer Group, Williamsburg, VA, December 1997.
17. Williams, S., “Superpave Mix Designs for Arkansas”, MS Thesis, University of Arkansas, Fayetteville, Arkansas, 1998.
18. Ng, H., “Effect of Void Size, Arrangement and Interconnectivity on Permeability of Hot-Mix Asphalt Concrete”, MS Thesis, University of Arkansas, Fayetteville, Arkansas, 1999.

APPENDIX A

Mix Properties

Location (source)- Virginia round robin testing

Compaction- Gyratory

Nominal Maximum Aggregate Size- 12.5 mm

Location (source)- Highway 22 Dardanelle

Compaction- Field

Nominal Maximum Aggregate Size- 12.5 mm

Binder Content- 5.80%

Aggregates- a) 3/4", Duffield Quarry, Russelville

b) Washed 3/8", Duffield Quarry, Russelville

c) No. 4, Duffield Quarry, Russelville

d) Sand, Duffield Quarry, Russelville

e) Rescreened Screenings, Duffield Quarry, Russelville

Location (source)- Highway 286 Greenbrier Job # 080130

Compaction- Field

Nominal Maximum Aggregate Size- 12.5 mm

Binder Content- 5.80%

Aggregates- a) 5/8" chips, Rogers Group, Greenbrier

b) Screenings, Rogers Group, Greenbrier

c) Sand, Rogers Group, Greenbrier

d) Ind. Sand, Rogers Group, Greenbrier

e) LSD, Batesville Lime, Batesville

Location (source)- Springdale 71-B, Sta. 143+90, 147+00, 151+50, 153+44, 148+70

Compaction- Field

Nominal Maximum Aggregate Size- 12.5 mm

Binder Content- 6.20%

Aggregates- a) 3/4", Preston Quarry, Van Buren

b) 1/2", LS Sharps Quarry, Lowell

c) HDS, Humble Pitcher, Ok

d) Screenings, West Fork Quarry, West Fork

Location (source)- Highway 45, Hartford, Sta. 102+50, 99+50, 92+50,

Compaction- Gyratory

Nominal Maximum Aggregate Size- 12.5 mm

Binder Content- 6.30%

Location (source)- Highway I-40 Morgan, Sta. 850+41

Compaction- Gyratory

Nominal Maximum Aggregate Size- 12.5 mm

Binder Content- 5.20%

Aggregates- a) STO 164, Granite Mountain Quarry, Sweet Home

b) STO 163, Granite Mountain Quarry, Sweet Home

c) STO 162, Granite Mountain Quarry, Sweet Home

Location (source)- Freshour, Cabot

Compaction- Gyratory

Nominal Maximum Aggregate Size- 12.5 mm

Binder Content- 5.20%

Aggregates- a) 1 1/4", Cabot Quarries, Cabot

b) 2 3/4" Minus, Cabot Quarries, Cabot

c) 3 5/8", Chip, Cabot Quarries, Cabot

d) Industrial Sand, Granite Mountain, Little Rock

e) #4 Fill, Cabot Quarries, Cabot

f) Donna Fill, 3 M, Little Rock

Location (source)- Jenny Lind, Arkhola

Compaction- Gyratory

Nominal Maximum Aggregate Size- 12.5 mm

Binder Content- 6.1%

Aggregates- a) 3/4", Arkhola, Jenny Lind

b) 1/2" Chips, Arkhola, Jenny Lind

c) 3/8", GR Chips, Arkhola, Van Buren

d) 1/4", Screenings, Arkhola, Jenny Lind

e) 1/4", Washed PRSTN, Preston Quarry, Van Buren

f) BH Fines, Arkhola, Jenny Lind

Location (source)- Lowell, McClinton-Anchor

Compaction- Gyratory

Nominal Maximum Aggregate Size- 25 mm

Binder Content- 5.20%

Aggregates- a) 1 1/2" LS, Sharps Quarry, Lowell

b) 1/2" LS, Sharps Quarry, Lowell

c) HDS, Humble, Pitcher, Ok

d) WF Screenings, West Fork Quarry, West Fork

APPENDIX B

Specimen Preparation and Permeability Test Instructions

Referenced Documents- The following AASHTO Standards are used as part of the experimental procedures:

- 1) T 166 Bulk Specific Gravity of Compacted Bituminous Mixtures
- 2) T 209 Maximum Specific Gravity of Bituminous Paving Mixtures
- 3) T 269 In-place Air Voids of Compacted Dense and Open Bituminous Paving Mixtures
- 4) T 283 Resistance of Compacted Bituminous Mixture to Moisture Induced Damage

Apparatus- The following apparatus/instruments were used:

- 1) Vacuum container, Type E from AASHTO T 209, and vacuum pump from AASHTO T 209 (including the respective manometer).
- 2) Specimen spacer from AASHTO T 283.
- 3) Balance and water bath from AASHTO T 283.
- 4) Supply of distilled water at $23 \pm 2^\circ \text{C}$.
- 5) Supply of petroleum-based sealant or grease (e. g. K-Y Jelly, Vaseline).
- 6) Karol-Warner Flexible Wall Permeameter (including its standpipe, i.e. graduated cylinder).
- 7) Stopwatch.
- 8) Timer.
- 9) Meterstick.
- 10) Digital Caliper.
- 11) Straight-edge.

Preparation of Test Specimens- If the percentage of air voids in the specimen is not known, the following procedure must be done *prior* to permeability testing:

- Determine the bulk specific gravity of the specimen according to AASHTO T-166
- Obtain the maximum specific gravity for the mix by the most applicable method available, e.g. construction records, direct measurement by AASHTO T-209 using a companion “loose” mix sample, etc.
- Determine the air void content of the specimen according to AASHTO T-269.

The following steps were followed when preparing each of the samples for permeability testing:

- 1) The height (thickness) of the specimen was measured using a digital caliper and recorded. The height of the specimen used in the calculations for hydraulic conductivity is the average of four (4) measurements taken at different locations (separated by 90 degrees around the circumference of the sample, making them equidistant). Each measurement was taken at approximately 1 cm inward from the outside edge. The height was recorded on a data sheet, to the nearest 0.001 cm (refer to Appendix 3).
- 2) The diameter of the specimen was measured and recorded in the same fashion as the height (refer to Appendix 3).
- 3) The specimen was placed in a horizontal position in the vacuum container supported above the container bottom by the spacer. The container was then filled with distilled water at room temperature so that the specimens had at least 25 mm of water above their surface.
- 4) *Vacuum Saturation*- In order to remove trapped air and to ensure total specimen saturation, a vacuum was gradually applied until the residual (negative gage) pressure on

the manometer read 28 ± 2 mm of Hg. This residual pressure was maintained for 15 ± 2 minutes. During vacuum saturation the container was manually agitated at 2-minute intervals by applying 12 taps of a rubber mallet (3 taps at each of 4 different locations separated approximately 90 degrees around the perimeter of the container).

- 5) At the end of the vacuum saturation period, the vacuum was released by slowly increasing the pressure.
- 6) The specimen was then let to stand undisturbed for 5 to 10 minutes.
- 7) In order to observe the effect of the 15 minute vacuum saturation period, the saturated, surface dry mass (SSD mass) was obtained according to AASHTO T 166 and compared to the SSD mass obtained by the bulk specific gravity calculation previously done.
- 8) After determining the SSD mass, the specimen was returned to the vacuum container and left submerged until ready for testing.

Permeameter calibration/verification

Calibration of the permeameter used must be done prior to testing. However, once initial calibration has been performed and the permeameter has been assembled for testing, further calibration is not necessary. The following steps were followed for the calibration of the permeameter used:

- 1) The standpipe tube (graduated transparent cylinder) was removed from the permeameter.
- 2) Using the meterstick, 13.8 mm were measured from the end of the tube and a mark was placed.
- 3) The inside diameter was measured using the digital calipers. This diameter was measured as 3.166 cm.

- 4) An upper mark was established by first calculating the distance between marks for a water volume of 500 ml. Then, using the meter, this distance was measured off and marked. The following equation was used to calculate the distance required for 500 ml volume:

$$h_{req} = \frac{4 \times 500}{\pi d^2} \quad \text{(Equation 14)}$$

where h_{reqd} = height (cm) required for 500 ml volume.

d = diameter of the pipe (cm).

Using the 3.166 cm inner diameter of the standpipe and Equation 14, the upper mark was found to be at 63.51 cm above the zero mark.

- 5) Once the upper and lower (zero) timing marks were established, the standpipe was reinserted into the upper confinement plate of the permeameter.

If the permeameter standpipe has manufacturer established timing marks, then steps 1 through 4 should be done to ensure that the timing marks have been properly positioned.

Testing Procedure-

The same procedure was done on all samples tested in phase I of this research. A detailed description follows.

- 1) In order to begin, the permeameter specimen cylinder was disassembled from the permeameter base.
- 2) The pressure line of the permeameter was connected to the vacuum side of the pump.

Using the pump, a vacuum was applied to the flexible wall (latex rubber membrane) to

remove entrapped air and collapse the membrane against the inside diameter of the cylinder. This facilitated the loading of the samples.

- 3) The specimen was then removed from the vacuum container filled with distilled water. As quickly as possible, a liberal coating of sealant (Vaseline) was applied to the sample's side surface. Extreme care was taken to ensure that sealant penetrated the air voids on the sample's side surface; however, care was also taken towards preventing the presence of any sealant on the top or bottom surfaces of the specimen. Any excess sealant was removed using a straight-edge.
- 4) The specimen was placed on the base of the permeameter.
- 5) The following steps were followed to assemble the permeameter. First, the top plate of the permeameter is placed on the top surface of the sample. Second, the metal cylinder (to which the flexible wall is attached) is positioned over and around the sample and the top plate. The top plate, the sample, and the rest of the permeameter were clamped together. All connections must be made at least finger-tight. All plate springs, such as the springs of the upper specimen containment plate, should be compressed.
- 6) The pressure line was disconnected from the pressure line from the vacuum side of the pump and connected to the pressure side.
- 7) Using the pump, a confining pressure of 10 ± 1 psi was applied. All fluctuations in confining pressure were observed. Variations may be the result of insufficient seal or a hole in the flexible membrane. Care was exercised to ensure that the confining pressure remained constant throughout the test. If fluctuations persisted, steps 5 and 6 were meticulously repeated.
- 8) The permeameter was placed into a tared pan able to collect a minimum of 1000 ml.

- 9) The permeameter's reservoir tube was filled to the upper timing mark with distilled water at room temperature. This step must be done carefully so that the incorporation of air bubbles is minimized.
- 10) The permeameter was then leaned from side to side to allow the escape of any entrapped air. This operation was continued until "all" entrapped air had been removed.
- 11) Additional water was poured into the cylinder if necessary to bring the level back up to the upper timing mark.
- 12) The valve on the underside of the permeameter was opened to commence flow.
- 13) The water flow was observed and the total time it took for the head to fall from the 63.51 cm to the zero marks was recorded. If the time it took for the water head to drop from 63.51 cm to 0 cm was more than approximately 5 minutes, more than one reading was taken. Readings were taken at four different time intervals. Proper scaling was required so as to achieve time length consistency between readings. For instance, if the time it took for all 500 ml of water to flow through the sample was 20 minutes, then readings were taken at 5, 10, 15, and 20 minutes. If the test lasted longer than an hour, readings were taken at 15, 30, 45, and 60 minutes. No samples, other than a very few tested in the earliest stages of this research, were tested for more than one hour. Care was taken to ensure that the valve was closed at the moment the water dropped to the zero mark. If the valve is not closed and water is allowed to flow freely so that no hydraulic head is present on the sample, the water in the voids flows out, reducing the sample's percent saturation. This, in turn, affects the hydraulic conductivity (it is generally accepted that the hydraulic gradient is directly proportional to the saturation of a porous medium).

- 14) The permeameter was removed from the tared pan. The mass of water in the pan was measured and recorded. Afterwards, the water was discarded and the pan was thoroughly dried with a towel. The pan was re-tared. NOTE- The water mass collected on the pan was recorded only for the first 8 samples tested (samples provided by the Virginia Transportation Research Council for a round robin initial study executed by the ASTM Committee D-4).
- 15) Steps 8 through 14 were repeated four additional times.
- 16) Using the vacuum pump in the Karol-Warner Flexible Wall Permeameter, the confining pressure was increased to 14±1 psi. Steps 8 through 15 were repeated five times for the increased confining pressure.
- 17) The specimen was removed from the permeameter and retained for future testing.

Note- After several permeability tests are performed on the same specimen, the petroleum based sealant (Vaseline) tends to deteriorate the conditions of the latex rubber membrane. To prevent leaks that would result in unstable confining pressures and/or water “short-circuiting” the asphalt samples, membranes should be replaced as often as supply permits.

Calculation

During the test, the SSD mass after vacuum, timing mark distances, flow times, and water mass measurements (for initial samples) were recorded. The permeability (hydraulic conductivity) of the samples tested was calculated using Equation 12.

$$k = 2.303 \frac{al}{At} \log_{10} \left(\frac{h_1}{h_2} \right)$$

In this case, a , the cross-sectional area of the pipe was calculated to be 10.024 cm² from the following simple calculation:

$$a = (\pi \times d^2)/4 \text{ where } d = \text{diameter of the pipe in cm (3.166 cm)}$$

For simplicity, a spreadsheet that performs the necessary calculations as shown in Equation 12 was created (refer to Appendix 4 for typical sample calculations).

Report

For further data analysis, the permeability of the test specimen in units of 10^{-5} cm/sec, the height (thickness) of the specimen, and the percent air voids to the nearest 0.1 percent were recorded.

APPENDIX C

Laboratory Performance Testing Using ERSA

ERSA Set Up and Run

1. Wire up samples. (Place steel plate cross-wise for field slabs and length-wise for gyratory samples.) Be sure wires are tight.
2. Spray sample trays with WD-40 and line with trash bag.
3. Place filler blocks around sample and set sample in tray to make sure everything fits (i.e. sample is not touching filler blocks.). Sample should be spaced evenly from side to side and about 1 - 1/4" from the front of the sample tray.
4. Mix plaster. (Need 2 plastic buckets, water, plaster, mixer, paddle, spoon, and metal pail)
Proportion: ~1/2 bag of plaster to 2/3 pail of water. Plaster should be thick enough to barely cover your hand without skin showing through.
5. Pour plaster into molds around sample making sure that level of plaster is up to edge of sample trays.
6. Let samples sit for several hours or overnight.
7. Use engine lift to set samples into ERSA. Bolt 4 bolts for each sample. (Sample 1 or 3 goes on left side, and sample 2 or 4 goes on right side.)
8. Be sure valve on back of recirculation unit is closed and filter has been replaced.
(Replace filter when dirty.)
9. Plug in ERSA (orange extension cord from back of ERSA).
10. Let water run in sink until hot.
11. Turn water off and drag green water hose into ERSA.

12. Turn hot water to 9:00 and cold water to 11:00.
13. When water in ERSA tanks is above the level of suction, turn on recirculation unit. It will bubble at first, then should settle down. (If not, tighten filter.)
14. When samples are halfway filled with water, place thermometer in water. Temp. should be 55 – 60 C.
15. Let water fill to about 1” to 1-1/2” above samples. Turn water off and remove water hose.
16. When water temp reaches 53 C, close lid and let samples soak for at least 4 hours (or until water temperature reaches 50 C.)
17. Set up computer – Double click on Workbench.exe icon.
 - File – Open -- ERSA.wbw
 - Double click on Write01 icon in top right corner.
 - Click File Name... in lower right corner.
 - Enter file name from index card.-- OK -- OK
18. When samples are ready to start, add weights (9 on each side), turn ERSA on, let it run 5 – 10 cycles, then press play button on computer screen (top left corner).
19. Let ERSA run for at least 20,600 cycles. (about 19 hours)
20. Press stop button on computer screen.
21. Turn ERSA off.
22. File exit and save changes.
23. Save file to disk (from C: \wbfw\filename.asc)
24. Remove weights.

25. Drag drain hose out the brown door (aimed away from the door) and open valve in back of recirculation unit.
26. Unbolt samples and set in floor.
27. Turn off recirculation unit, change filter (being careful not to lose the black O-ring), and put hose back in bucket.
28. Close valve in back of recirculation unit.
29. Vacuum out remaining water with Shop-Vac until completely dry. (Empty Shop-Vac outside.)
30. Clean wheels with naphtha.
31. Unplug ERSA and close lid.
32. Disassemble sample trays, clean, and reassemble.